

DETERMINATION OF WATER TRANSPORT NUMBERS
IN CATION EXCHANGE MEMBRANES BY AN EMF
(STREAMING POTENTIAL) METHOD.

BY

CHARLES OTIENO ONINDO

A Thesis submitted in partial fulfilment for the
Degree of Master of Science in Kenyatta University.

OCTOBER, 1987.

Owindo, Charles
*Determination of
water transport*



89/185166

This Thesis is my original work and has not been presented for a degree in any other University.

Onindo

CHARLES OTIENO ONINDO
KENYATTA UNIVERSITY

This Thesis has been submitted for examination with my approval as University Supervisor.

H. M. Thairu

(PROFESSOR HENRY M. THAIRU)
DEPARTMENT OF CHEMISTRY
KENYATTA UNIVERSITY

ACKNOWLEDGEMENTS:

I wish to express special appreciation for the inspiration and wise counsel I received from Professor Henry Thairu, my supervisor, during the entire period of my investigations. His assistance, guidance, suggestions and invaluable advice contributed to the success of the entire work.

My thanks also go to Professor Naftali Muriithi, Chairman, Department of Chemistry whose help made these studies possible. I also wish to acknowledge with thanks the support I got from the entire technical staff of the department of chemistry.

I am indebted to Kenyatta University for offering me the scholarship and thus providing the funds for my study.

I am also thankful to Ms. Mary Shumwe for her painstaking help with typing the manuscript.

Lastly I wish to express my sincere thanks to all those who made this work possible in one way or another.

TABLE OF CONTENTS

	<u>Page</u>
ABSTRACT:	vii
<u>CHAPTER 1</u>	1
1.1 Introduction	1
1.2 Objectives	2
1.3 Scope	3
1.4 Organization of the report	4
1.5 Summary	5
<u>CHAPTER 2</u>	6
2.1 Literature Review	6
2.2 Theoretical background	10
2.2.1 Stress-strain relationship	10
2.2.2 Yield point phenomenon	11
2.2.3 Strain rate sensitivity	12
2.2.4 Work hardening	13
2.2.5 Strain rate effect on yield strength	14
2.2.6 Strain rate effect on ultimate tensile strength	15
2.2.7 Strain rate effect on elongation	16
2.2.8 Strain rate effect on reduction of area	17
2.2.9 Strain rate effect on fracture toughness	18
2.2.10 Strain rate effect on impact strength	19
2.2.11 Strain rate effect on creep	20
2.2.12 Strain rate effect on fatigue	21
2.2.13 Strain rate effect on fracture	22
2.2.14 Strain rate effect on fracture toughness	23
2.2.15 Strain rate effect on fracture toughness	24
2.2.16 Strain rate effect on fracture toughness	25
2.2.17 Strain rate effect on fracture toughness	26
2.2.18 Strain rate effect on fracture toughness	27
2.2.19 Strain rate effect on fracture toughness	28
2.2.20 Strain rate effect on fracture toughness	29
2.2.21 Strain rate effect on fracture toughness	30
2.2.22 Strain rate effect on fracture toughness	31
2.2.23 Strain rate effect on fracture toughness	32
2.2.24 Strain rate effect on fracture toughness	33
2.2.25 Strain rate effect on fracture toughness	34
2.2.26 Strain rate effect on fracture toughness	35
2.2.27 Strain rate effect on fracture toughness	36
2.2.28 Strain rate effect on fracture toughness	37
2.2.29 Strain rate effect on fracture toughness	38
2.2.30 Strain rate effect on fracture toughness	39
2.2.31 Strain rate effect on fracture toughness	40
2.2.32 Strain rate effect on fracture toughness	41
2.2.33 Strain rate effect on fracture toughness	42
2.2.34 Strain rate effect on fracture toughness	43
2.2.35 Strain rate effect on fracture toughness	44
2.2.36 Strain rate effect on fracture toughness	45
2.2.37 Strain rate effect on fracture toughness	46
2.2.38 Strain rate effect on fracture toughness	47
2.2.39 Strain rate effect on fracture toughness	48
2.2.40 Strain rate effect on fracture toughness	49
2.2.41 Strain rate effect on fracture toughness	50
2.2.42 Strain rate effect on fracture toughness	51
2.2.43 Strain rate effect on fracture toughness	52
2.2.44 Strain rate effect on fracture toughness	53
2.2.45 Strain rate effect on fracture toughness	54
2.2.46 Strain rate effect on fracture toughness	55
2.2.47 Strain rate effect on fracture toughness	56
2.2.48 Strain rate effect on fracture toughness	57
2.2.49 Strain rate effect on fracture toughness	58
2.2.50 Strain rate effect on fracture toughness	59
2.2.51 Strain rate effect on fracture toughness	60
2.2.52 Strain rate effect on fracture toughness	61
2.2.53 Strain rate effect on fracture toughness	62
2.2.54 Strain rate effect on fracture toughness	63
2.2.55 Strain rate effect on fracture toughness	64
2.2.56 Strain rate effect on fracture toughness	65
2.2.57 Strain rate effect on fracture toughness	66
2.2.58 Strain rate effect on fracture toughness	67
2.2.59 Strain rate effect on fracture toughness	68
2.2.60 Strain rate effect on fracture toughness	69
2.2.61 Strain rate effect on fracture toughness	70
2.2.62 Strain rate effect on fracture toughness	71
2.2.63 Strain rate effect on fracture toughness	72
2.2.64 Strain rate effect on fracture toughness	73
2.2.65 Strain rate effect on fracture toughness	74
2.2.66 Strain rate effect on fracture toughness	75
2.2.67 Strain rate effect on fracture toughness	76
2.2.68 Strain rate effect on fracture toughness	77
2.2.69 Strain rate effect on fracture toughness	78
2.2.70 Strain rate effect on fracture toughness	79
2.2.71 Strain rate effect on fracture toughness	80
2.2.72 Strain rate effect on fracture toughness	81
2.2.73 Strain rate effect on fracture toughness	82
2.2.74 Strain rate effect on fracture toughness	83
2.2.75 Strain rate effect on fracture toughness	84
2.2.76 Strain rate effect on fracture toughness	85
2.2.77 Strain rate effect on fracture toughness	86
2.2.78 Strain rate effect on fracture toughness	87
2.2.79 Strain rate effect on fracture toughness	88
2.2.80 Strain rate effect on fracture toughness	89
2.2.81 Strain rate effect on fracture toughness	90
2.2.82 Strain rate effect on fracture toughness	91
2.2.83 Strain rate effect on fracture toughness	92
2.2.84 Strain rate effect on fracture toughness	93
2.2.85 Strain rate effect on fracture toughness	94
2.2.86 Strain rate effect on fracture toughness	95
2.2.87 Strain rate effect on fracture toughness	96
2.2.88 Strain rate effect on fracture toughness	97
2.2.89 Strain rate effect on fracture toughness	98
2.2.90 Strain rate effect on fracture toughness	99
2.2.91 Strain rate effect on fracture toughness	100
2.2.92 Strain rate effect on fracture toughness	101
2.2.93 Strain rate effect on fracture toughness	102
2.2.94 Strain rate effect on fracture toughness	103
2.2.95 Strain rate effect on fracture toughness	104
2.2.96 Strain rate effect on fracture toughness	105
2.2.97 Strain rate effect on fracture toughness	106
2.2.98 Strain rate effect on fracture toughness	107
2.2.99 Strain rate effect on fracture toughness	108
2.2.100 Strain rate effect on fracture toughness	109

Dedicated to my mother and father

TABLE OF CONTENTS:

	<u>PAGE.</u>
ABSTRACT:	vii
<u>CHAPTER 1:</u>	
1. Introduction	1
<u>CHAPTER 2:</u>	
2. Literature Review	4
2.1 Electroosmotic Method	4
2.2 Streaming potential	9
2.3 Theoretical Framework for this study	13
2.3.1 Application of irreversible thermodynamics to a system having pressure gradient	14
<u>CHAPTER 3:</u>	
3. Experimental	20
3.1 Calibration of glassware	20
3.2 The Apparatus	22
3.2.1 The Cell	22
3.2.2 The Pressure source	23
3.2.3 General Apparatus handling	23
3.3 The Electrodes	26
3.4 Solutions	31

	<u>PAGE:</u>	
3.5	Membranes	31
3.6	Experimental Procedures	32
3.6.1	Streaming Potential measurements in Permaplex C-20	32
3.6.1.1	Repeat of Streaming potential measurements in Permaplex C-20	33
3.6.2	Streaming Potential Measurements in Nepton CR 61 AZL 065 and Nepton CR 61 AZL 183	34
3.6.3	Streaming Potential Measurements in BDH Cation Exchange Membrane	34
3.6.4	Addition of Silver Nitrate to Experimental Solutions	36
3.7	Measurements	37
 <u>CHAPTER 4:</u>		
4.	Results and Calculations	46
 <u>CHAPTER 5:</u>		
5.	Discussion and Conclusion	62
 <u>APPENDICES:</u>		
A.1	Calculation of densities of electrolyte solutions at 25°C	70
	REFERENCES	73

ABSTRACT:

The work presented is an experimental determination of water transport numbers as a function of concentration of electrolytes in some cation exchange membranes. These were Permaplex C-20, BDH (Na^+ form), Nepton CR 61 AZL 065 and Nepton CR 61 AZL 183 membranes.

Experimental investigation is done in the following cell with cation exchange membrane at a temperature of 25°C .

CATION

$\text{Ag}/\text{AgCl}/\text{MCl}(\text{aqC}_1)/\text{EXCHANGE}/\text{MCl}(\text{aqC}_1)/\text{AgCl}/\text{Ag}$
MEMBRANE

This is done for the aqueous electrolyte solutions MCl , where M is the alkali metal cation Li^+ , Na^+ and K^+ . Thus Sodium Chloride, Lithium Chloride and Potassium Chloride are studied.

An approach based on the theory of irreversible thermodynamics is used to derive an equation of the emf of the cell. The equation is used to calculate the water transport numbers.

Silver - Silver Chloride electrodes are prepared and used for the measurements of the streaming potentials. On application of short hydrostatic pressure pulses lasting 4.5 seconds, the streaming potential is measured as a function of time and recorded as square pulses.

The experimental water transport numbers are observed to be decreasing with increasing concentration of solutions within the concentration range of 0.1M to 1M of electrolytes studied.

Attempt is made to determine water transport numbers across the thin BDH(Na^+) membrane by mounting several pieces of the membranes in the cell. It is observed that the streaming potential method is yet not a good method for transport number determination in thin membranes.

CHAPTER 1:

1. Introduction.

Large amount of interesting work has been published in the last two decades showing considerable interest existing among chemists, chemical engineers and biologists in understanding the transport process occurring across artificial membranes separating different solutions. Chemists would like to understand the mechanism of transport so that with the knowledge so gained they would be able to fabricate membranes of any desired property or properties. Biologists however would like to use them as simple models for physiological membranes.

The electroosmotic and streaming potential methods have been used for the determination of water transport number. Water transport number (\bar{t}_w) is defined as the number of moles of water transported per Faraday across the membrane. When an electric field is applied to a membrane system

Anode/Solution(C_1)/Membrane/Solution(C_2)/Cathode

it causes not only transference of ions but also transference of liquid existing in the pores of

the membrane. This solvent transport accompanying ion transport through a membrane can be called in a phenomenological way electroosmosis. The solvent is carried by the counter-ions since the latter impart more momentum to the solvent than the co-ions do.

On the other hand when an excess hydrostatic pressure is applied to the solution on one side, the liquid in the pore of the membrane is displaced leading to the development of a potential called the streaming potential. The connection between electroosmosis and streaming potential has been known through Saxen relation (1). Saxen derived a number of relations which have been deduced by Mazur and Overbeek (2) from the phenomenological equations of irreversible thermodynamics thus demonstrating the validity of Saxen relation.

Brun and Vaala (3) pointed out that electroosmosis experiments can give erroneous results due to concentration polarization and

therefore the aim of this experimental study was mainly to obtain more accurate experimental water transport numbers by using a more reliable streaming potential method for some cationic exchanger membranes. However, the application of high pressures in streaming potential measurements by Trivijitkasem, P. and Østvold, T. (4) could have resulted in disturbing the membrane equilibria and hence application of low hydrostatic pressures in this experimental study would be preferred.

The main theoretical approach used to describe the emf of a galvanic cell with a cationic exchanger membrane have been reviewed in the next chapter on the Literature review. The approach used in the work is based on the principles of irreversible thermodynamics proposed by Førland and Thulin (5). Other aspects are considered in the work by Førland, Thulin and Østvold (6). In this work unmeasurable quantities like single electrode potentials have been avoided. Thus in the theoretical formulations, quantities that are thermodynamically well defined and which are measurable have been used.

CHAPTER 2.

2. Literature Review:

In this section a literature review will be given and then the postulates of irreversible thermodynamics and its application to the determination of water transport in cationic exchange membrane by an emf method.

2.1. Electroosmotic Method.

A great deal of work dealing with electroosmosis in ion exchanger membranes was reviewed by Lakshminarayanan (7). Water transport (\bar{t}_w) has been measured by various investigators using a variety of techniques and cell designs. Basically two methods, one based on weight changes and the other based on volume changes have been used. The weight method is accurate with flexible membranes which are likely to move back and forth during electrolysis.

The main noncontroversial results on water transport are as follows: Water transport (\bar{t}_w) decreases as the external concentration is increased and also as the water content of the membrane is **decreased.** The effect of crosslinked membrane matrix on water transport depended on

the way crosslinking affected the water content of the membrane. \bar{t}_w decreased in the order Cs=Rb<K < Na < Li. The transfer also decreased as the charge of the ion permeating the membrane increased. The specific binding of the ions to the fixed groups of the membrane become very important as the ionic charge increased.

Rosenberg, George and Potter (8) working with Nepton CR-61 membrane found that thorium counter-ion with an ionic charge of four gave a negative transport of water. This, they explained as being due to the ion so strongly adsorbed that it conferred anion selectivity to the membrane and thus water transported in the opposite direction. A similar case was reported by Schulz (9) this time using Permaplex A - 10 membrane. Adsorption of diphosphate anion reversed the direction of transport of water.

Oda and Yawataya (10) assumed the net transport of water for monovalent ions and negatively charged membranes to be given by.

$$\bar{t}_w = n_+ \bar{t}_+ - n_- \bar{t}_- \quad \dots\dots\dots 2.1.1$$

where n_+ and n_- are the number of moles of water associated with cation and anion respectively.

They found that \bar{t}_w values vary linearly with \bar{t}_+

(cation transport number) and that \bar{t}_w depended on the water content of the membrane. They also found out that the solution after having gone through the membrane was more concentrated in cation than the "bound water" existing in the membrane phase.

Winger et al (11) assumed as did Oda and Yawataya (10) that the net transport of water was given by:

$$\bar{t}_w = \bar{t}_+ \left[\frac{n_+}{z_+} + \frac{n_-}{z_-} \right] - \frac{n_-}{z_-} \dots\dots 2.1.2.$$

when n_+ and n_- are the number of moles of water associated with cation and anion respectively. They accordingly found a linear variation between \bar{t}_w and \bar{t}_+ the cationic transport number. Extending the straight line in either direction it was found that for $\bar{t}_+ = 1$, n_+ was 14.1, 8.6. and 7.3 for Li^+ , Na^+ and K^+ , respectively and for $\bar{t}_w = 0$, n_- for the OH ion was about 5 and \bar{t}_+ for the different species were $\text{LiOH} = 0.24$, $\text{NaOH} = 0.38$ and $\text{KOH} = 0.45$. These values were probably the solution transport numbers for the concentrated alkali solutions (~6M).

Kressman, Stanbridge, Tye and Wilson (12) working with Permaplex C-20 and T.N.O C-60 membranes and with the same solutions as Winger et al found that their plots of \bar{t}_w against \bar{t}_+ was curved but not linear. They related water transport to the transport number of the counter-ion by the expression.

$$\bar{t}_w = \bar{t}_+ (W + 1) - 1 \quad \dots\dots\dots 2.1.3.$$

where W was the moles of water per equivalent of counter-ion in the membrane and -1 and 1 mole are associated with OH⁻ group. This non-linearity was ascribed to the variation of W with external concentration. They however found \bar{t}_w calculated using equation 2.1.3 to agree with the \bar{t}_w values measured. The curved lines also appear to meet at a common intercept when the counter-ion transference was zero.

Tombalkian, Barton and Graydon (13) reported dependence of \bar{t}_w on current density. They found \bar{t}_w values to decrease at very high current density. Lakshminarayanaiah et al (14) using PSA and AMF C-103 membranes shows not only dependence but also independence of \bar{t}_w on current density. The dependence of \bar{t}_w on current density can result from some corresponding change in the structure of ion-solvent complex or more likely

in the distribution of ions and charges within the membrane. A further explanation may be that the variation of \bar{t}_w is the result of some chemical change in the membrane during electrolysis i.e. concentration polarization.

Mussini et al (15) made a test for water transport in a cell containing Na^+ , Cl^- and dioxane co-solvent with a cationic montmorillonite membrane. The transport of water was -6.5 ± 0.2 mole/Faraday with transport of water from cathode to anode.

Brun and Vaula (3) gave a mathematical treatment of polarization effect during electroosmotic measurements. Their conclusion was that apparent experimental values for the electroosmotic coefficients in dilute systems may be in error even if they are independent of current density. They suggested an extrapolation method for correcting for polarization effects.

Although much work has been done on water transport using electroosmotic method, it is evident that electroosmotic method has some inherent problems that have not been fully explained. There seems to be no well founded justification for taking \bar{t}_w at high

current densities as more valid than those at low current densities. However, it would be of interest to see how much has been done using the streaming potential method.

2.2. Streaming potential:

Applying an excess of hydrostatic pressure to the solution of one side of a cell of the type shown in Fig. 1.1 creates a potential called streaming potential. Its magnitude can be measured using suitable electrodes i.e. silver/silver chloride electrodes.

Helffferich (16) reviewed the work of Schmid and Schwarz (17;18). Assuming the absence of concentration gradient within the membrane and of specific interaction between the mobile species and the fixed group of the membrane, it is shown that the streaming potential $\Delta\Psi$ is related to the hydrostatic pressure ΔP by the relation

$$\Delta\Psi = \left(\frac{W\bar{X}F}{P_c \bar{K}} \right) \Delta P \quad \dots\dots\dots 2.2.1$$

where W was the sign of the fixed charges, P_c the flow resistance, \bar{X} the concentration of fixed charges and \bar{K} the conductivity of the membrane. $\Delta\Psi$ is directly proportional to ΔP and to \bar{X} but the effect of \bar{X} is annuled by the effect of \bar{K} . The membrane thickness

has no effect on the streaming potential whose magnitude is about a few millivolts for $\Delta P = 1$ atm across a typical ion exchanger.

Stewart and Graydon (19) studies the emf's of a concentration cell under conditions of constant pressure 1 atm on the dilute solution (0.05M) and of varying pressure upto 3 atm on the concentrated solution (0.1M) and observed the emf across each membrane to go above the theoretical value, but the increase was not much. Henderson (20) on the other hand studied the effect of applying pressure equally on both sides of the membrane cell (bi-ionic and concentration) employing both anion and cation exchange membranes. The change of potential with pressure was measured and found to vary linearly with pressure. The observed potential changes with pressure are all small and follow no set pattern.

Brun and Vaala (3) measured streaming potential in a system with phenolsuphonic acid, formaldehyde membranes and Potassium Chloride (KCl) and showed variation of potential with time. They obtained a mathematical expression for the potential dependence on time.

$$-\left(\frac{\Delta\phi}{\Delta P}\right) = \Delta\phi + A \int \frac{Dt}{\pi} \dots \quad 2.2.2$$

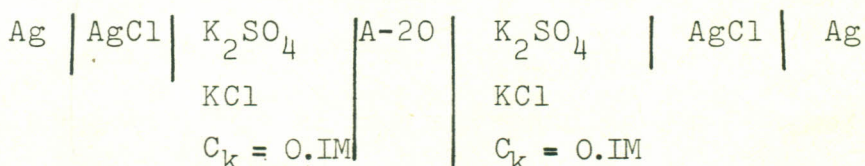
Here A is a constant, $\Delta\phi$ is the true streaming potential, t the time, π the number π and D is the salt diffusion coefficient.

Brun and Vaala (3) used the Saxen's relation as the basis for determining the electrokinetic cross-coefficient in their experimental work. But they pointed out that concentration polarization and membrane hydrolysis affected their results. They used the same membranes they previously used in 1957 (21) in the cell of the type used by Stewart and Graydon (19) for their streaming potential measurement. Potassium Chloride (KCl) solutions were studied. Square pulses ranging from 5 - 30cmHg pressure transmitted by gas and of duration of 70 seconds were applied alternatively on both sides. They observed that an initial rise was followed by a slower one. This was explained by reverse osmosis polarization. Plotting of this cell potential as a function of $t^{\frac{1}{2}}$ where t was time gave linear plots which could be extrapolated to zero to obtain more reliable value of streaming potential. They also suggested that shorter pulses could give better results.

Trivijitkasem and Østvold (4) obtained water transport numbers from streaming potential measurements for cation and anion exchange membranes. The pressure pulse was generated by nitrogen (N_2) gas using two electric valves. With this technique, they generated pressure pulses of upto $\Delta P = 1$ atm and measured streaming potential for even very dilute solutions.

The pressures were read from a manometer. After having applied pressure to one side of the membrane, a period of 5 - 10 minutes with atmospheric pressure on both sides was necessary to restore equilibrium conditions. The measurements were carried out at four concentrations, 0.001, 0.01, 0.1 and 1.0M of analytical grade inorganic salts LiCl, NaCl, KCl, RbCl and CsCl. Measurements were also carried out at 0.0005, 0.005, 0.05 and 0.5M concentrations of analytical grade inorganic salts MgCl₂, CaCl₂, SrCl₂ and BaCl₂. For analytical grade LaCl₃, measurements were carried out at 0.0003, 0.003, 0.03 and 0.3M concentrations.

Thairu (22) investigated the cell



He measured the streaming potential on application of hydrostatic pressure. The pressure source was the experimental solutions which were held in two glass reservoirs and where heights could be varied.

Identical results were obtained for all compositions investigated.

The work that has been done in this field is comparatively less when one considers the great extent of investigation of \bar{t}_w by electroosmotic method. Therefore, further work on water transport (\bar{t}_w) on cationic and anionic exchange membranes is necessary using the streaming potential method.

2.3. Theoretical Framework for this study:

The present theory of irreversible thermodynamics used in this work is based on the statistical mathematical investigation by Onsager (23). The theory is based on the following three postulates.

Postulate I: In a system where irreversible process takes place the thermodynamic state function exist and have the value which they would have if the system was in equilibrium e.g. in a system where there is a temperature gradient one can examine the thermodynamic properties of a very small volume element and find that they are the same as they would be if the surrounding parts of the system were at same temperature. For extremely large gradients in temperature or other intensive properties the postulate may not be valid.

Postulate II: The fluxes (J_i) are linear homogeneous functions of the forces (X_i), that is, any flux J_i can be expressed by an equation.

$$J_i = L_{i1}X_1 + L_{i2}X_2 + \dots + L_{ii}X_i \dots = \sum_j L_{ij}X_j$$

..... 2.3.1

where all the phenomenological coefficients L_{ij} are independent of the forces. The term $L_{ii}X_i$ is great compared to the term $L_{ij}X_i$ (where $i \neq j$) where all are due to coupling between different types of transport.

Postulate III: If linear relation between fluxes and forces are written as in equation (2.3.1), the following relation is valid for phenomenological coefficients

$$L_{ij} = L_{ji} \quad \dots\dots\dots 2.3.2.$$

This relation is known as the Onsager reciprocal relation.

2.3.1: Application of irreversible thermodynamics to a system having pressure gradient:

Consider a simple system of a cell with pressure difference over a membrane separating two half cells.

The temperature is assumed to be uniform over the system.

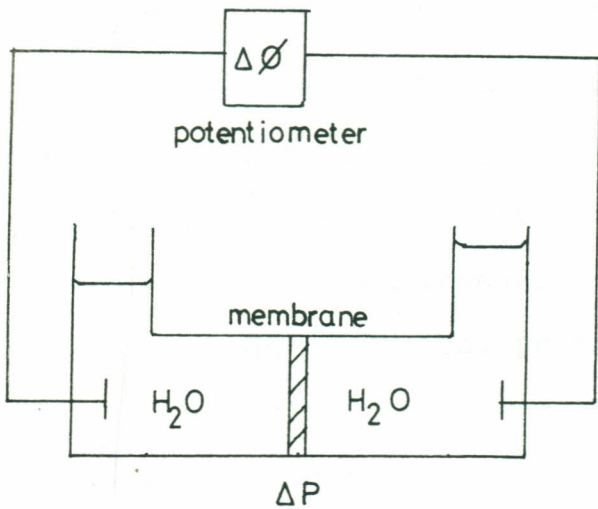


Fig. 2.3.1.

A simple case is a one component system e.g. H₂O (which dissociates slightly into ions). The electrode may e.g. be platinum on which hydrogen is absorbed forming hydrogen electrodes. The difference in chemical potential across the membrane is equal to $\Delta\mu^*_{H_2O} = V_{H_2O}\Delta P$ where V_{H_2O} is the molar volume of water. The dissipated energy per unit time can be written as

$$T\theta = \Delta P V_{H_2O} \frac{dn_{H_2O}}{dt} + \Delta\phi \cdot I \dots\dots 2.3.3$$

here $V_{H_2O} \frac{dn_{H_2O}}{dt} = J_v$ is the volume flux. It is further assumed that the volume change due to electrode reaction is negligible.

The phenomenological equations are written as

$$J_v = -L_{11} \Delta P - L_{12} \Delta \phi \quad \dots \quad (2.3.4)$$

$$I = -L_{21} \Delta P - L_{22} \Delta \phi \quad \dots \quad (2.3.5)$$

where according to Onsager $L_{12} = L_{21}$. Here is an irreversible volume transport due to pressure difference (ΔP) and an irreversible transport of charge due to an electrical potential difference ($\Delta \phi$). The interference of the two processes are given by coefficients L_{12} and L_{21} .

On the basis of equations (2.3.4) and (2.3.5), the pressure difference will create a potential difference, the streaming potential, defined as the potential difference per unit pressure difference for

$$I = 0 \quad \text{Thus} \quad \left(\frac{\Delta \phi}{\Delta P} \right)_{I=0} = \frac{-L_{21}}{L_{22}} \quad \dots \quad (2.3.6)$$

When $\Delta P = 0$, and dividing equation (2.3.4) by equation (2.3.5)

$$\left(\frac{J}{I}\right)_{\Delta P=0} = \frac{L_{12}}{L_{22}} \dots\dots\dots(2.3.7)$$

From Onsager reciprocal relations, equation (2.3.6) is equal to equation (2.3.7).

$$\text{T.h.us } \left(\frac{\Delta\phi}{\Delta P}\right)_{I=0} = - \left(\frac{J}{I}\right)_{\Delta P=0} \dots\dots\dots(2.3.8)$$

Further considering a cell with a multicomponent electrolyte and assuming that the composition of the electrolyte is the same on both sides of the membrane, so the difference in chemical potential (not including pressure) on the two sides is zero, $\Delta\mu_i = 0$. The energy dissipated will be

$$T.\theta = \Delta P \left(\sum_i \bar{V}_i \frac{dn_i}{dt} \right) + \Delta\phi.I \dots\dots\dots (2.3.9)$$

where $\bar{V}_i \frac{dn_i}{dt}$ is the volume flux. The flow in this multicomponent system (J_v) can be expressed by the flow of individual components, J_i , by the equation,

$$J_v = \sum_i \bar{V}_i J_i \dots\dots\dots (2.3.10).$$

The connection between e.g. the streaming potential and electroosmosis will be

$$\left(\frac{\Delta\phi}{\Delta P} \right)_{I=0} = - \left(\frac{J_v}{I} \right)_{\Delta P=0} = - \sum_i \left(\frac{J_i}{I} \right) \bar{V}_i = - \frac{1}{F} \sum_i t_i \bar{V}_i \dots\dots(2.3.11)$$

where t_i is the transport number of the neutral component measured by Hittorf type experiment and is dependent on the type of electrode used. Volume changes at the electrodes should also be included (ΔVel)

$$\left(\frac{\Delta\phi}{\Delta P} \right)_{I=0} = - \frac{1}{F} \left(\sum_i t_i \bar{V}_i + \Delta Vel \right) \dots\dots (2.3.12)$$

where ΔVel is the volume change at the right hand side of the electrode for each Faraday being transferred.

For the cell



The measured streaming potential, $\Delta\phi$, is given by

$$\Delta\phi = E = -\frac{1}{F} \left\{ t'_{\text{MCl}} \bar{V}_{\text{MCl}} + t'_{\text{H}_2\text{O}} V_{\text{H}_2\text{O}} + V_{\text{Ag}} - V_{\text{AgCl}} \right\} \Delta P$$

..... (2.3.13)

where $t'_{\text{MCl}} = 1$, \bar{V}_{MCl} , $V_{\text{H}_2\text{O}}$, V_{Ag} , V_{AgCl} are known, the

streaming potential, $\Delta\phi$, and pressure difference,

ΔP , are experimentally determined. The remaining

unknown $t'_{\text{H}_2\text{O}} = \bar{t}_w$, the water transport number,

can then be calculated from equation (2.3.13).

CHAPTER 3:

3. Experimental:

3.1. Calibration of glassware:

The accuracy of the commercially calibrated volumetric flask were verified before being put into use in this experimental work. To calibrate 200ml, 1000ml and 2000ml class A flasks, first the flasks were cleaned thoroughly and dried. The flasks were weighed using the substitution method of weighing as precise analytical balance could not be employed. Bosch S 2000 analytical balance weighs upto 200g. The flasks were filled to a few millimeters above the graduation line with distilled water which had been allowed to reach temperature equilibrium with both the room and the flasks. The base of the meniscus to the graduation line was set by removing the excess water with the aid of a teat pipette. The filled flasks were reweighed, water temperature and air temperature recorded. The water temperature was 24°C. The weight of water contained in the flasks were corrected to obtain the volume of the flasks at 20°C. Correction (in g) to be added to weight (in g) of distilled water at 24°C.

to obtain volume (ml) of vessel at 20°C for 1000ml nominal capacity was 3.69 (24). The corrections required for 200ml and 2000ml flasks were determined on a proportional basis. Density of water at 20°C corrected for buoyancy = 1.00284g/ml.

The average values of volumes were as follows:-

200	±	0.03ml
1000	±	0.04ml
2000	±	0.08ml

Calibration of glassware was done at 20°C because they were factory calibrated originally at 20°C.

3.2. The Apparatus:

3.2.1. The Cell:

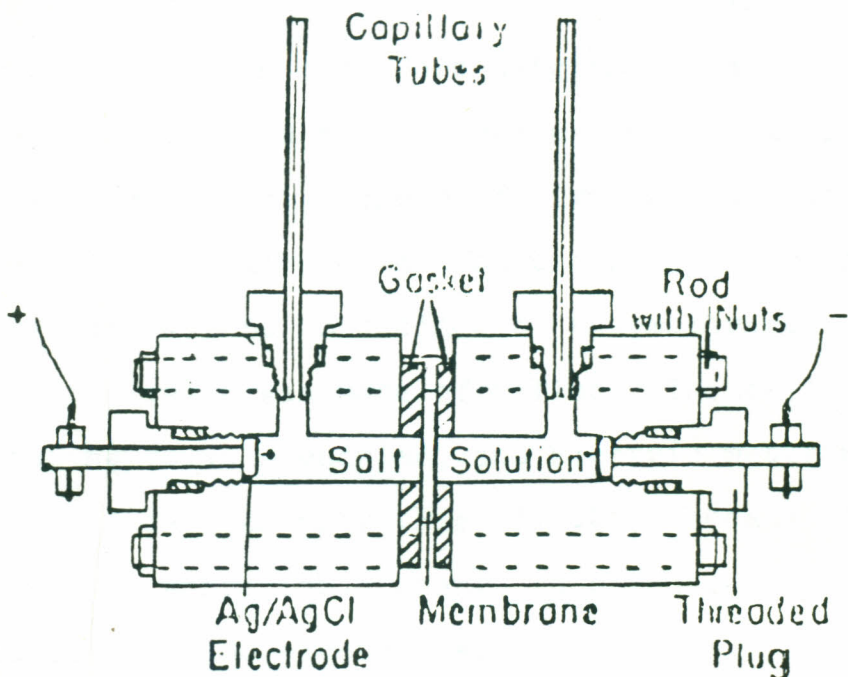


Fig. 3.2.1. - The cell for the measurement of streaming potential .

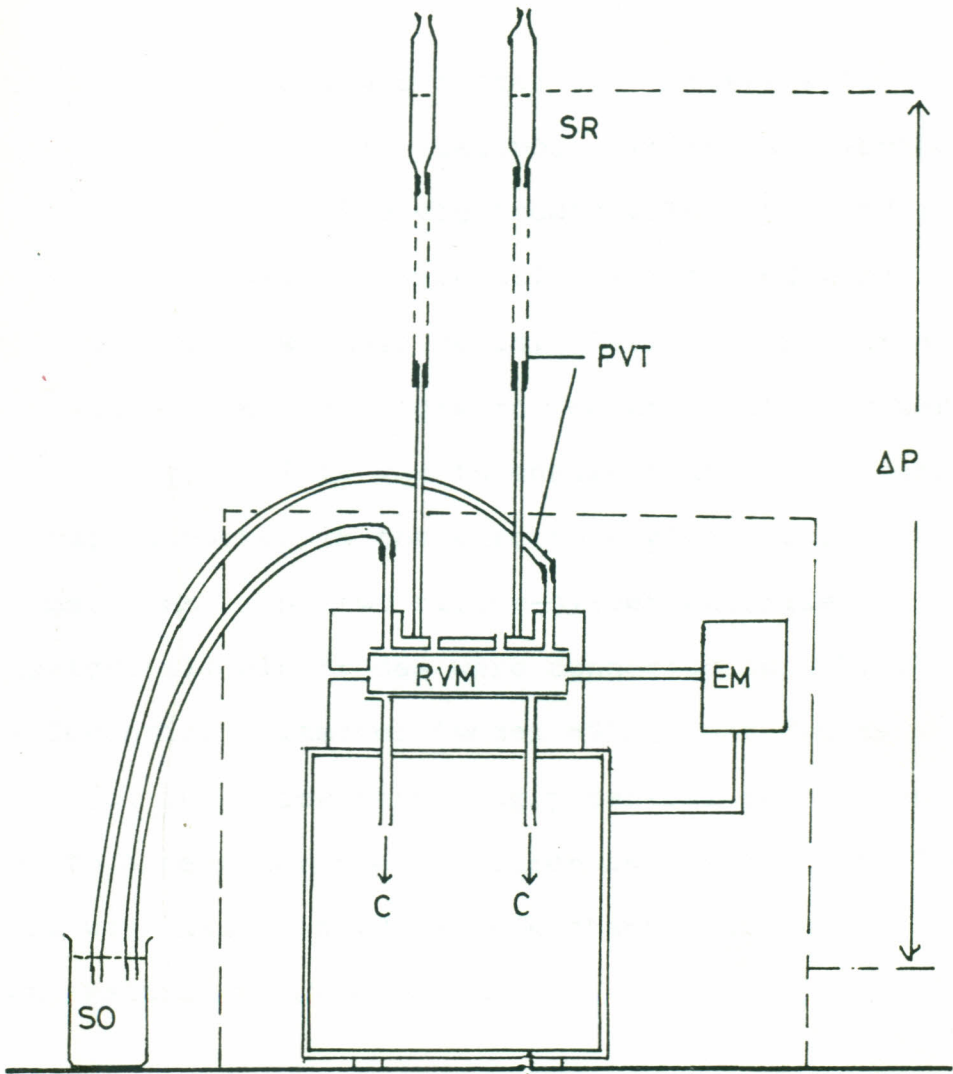
The cell used for the measurement of streaming potential was constructed as shown in Fig.3.2.1. It was similar to that used by Stewart and Graydon (25). The cell framework was made of plexiglass. The diameter of the exposed membrane was 0.5cm.

3.2.2. The Pressure source.

The cell was connected to the pressure source by PVC tubes in Fig. 3.2.2. The pressure source was the experimental solution which were held in two glass reservoirs and where heights could be varied. The motor rotated a valve mechanism through a series of gear wheels at a speed of five revolutions per minute. The valve mechanism distributed pressure alternatively to both sides of the membrane. This rotating valve was made of teflon. The cell, Rotating valve mechanism, and Electric Motor were put in a dark chamber (Fig. 3.2.2.) because light causes an appreciable change in potential of silver-silver chloride electrodes.

3.2.3. General Apparatus handling.

A circular piece of membrane was inserted in the cell. Maximum care was excercised in ensuring that grease from hands did not stain the exposed piece of membrane. To prevent any pressure leakage, high vacuum grease was applied in between the gaskets holding the membrane. The two half cell were then fixed together tightly to ensure that only electrical connection between the two half cells was through the membrane.



SR - Solution reservoirs.

PVT -PV tubes.

ΔP - Pressure difference between the membrane sides.

RVM- Rotating valve mechanism

EM - Electric motor connected to gear wheels.

SO - Solution overflow.

C - Cell for water transference.

Fig. 3.2.2. - Apparatus arrangement for measurement of streaming potential.

Each half cell was fitted with silver-silver chloride ($\text{Ag}/\text{AgCl}(\text{s})$) electrode which is described in section 3.3. The electrodes were supported in glass tubes (7mm in diameter) which fitted very well into the two half cells. Gaskets were put at the end of the electrodes to ensure that they were liquid tight. This was to ensure that no pressure leakage occurred in the electrode glass tubes connections. The two silver-silver chloride ($\text{Ag}/\text{AgCl}(\text{s})$) electrodes were connected to a D.C. differential voltmeter (model 895A, John Flukes mfg. Co; Inc.) for streaming potential measurements and to a recorder (Perkin Elmer 561 Recorder). The cell was placed inside a dark chamber at a temperature of about 25°C .

3.3. The Electrodes:

Silver-silver chloride electrodes ($\text{Ag}/\text{AgCl}(\text{s})$) used for the measurement of streaming potential for water transport number determination consisted of platinum wires as the electrode bases. The platinum wires were fused on to copper wires. A seal was made between the glass and platinum wire to make it liquid tight. While in the flame the wire was rotated to prevent the glass bead from flowing to one side and becoming eccentric. Melting proceeded from one end of the wire to avoid trapping air bubbles between the metal and glass.

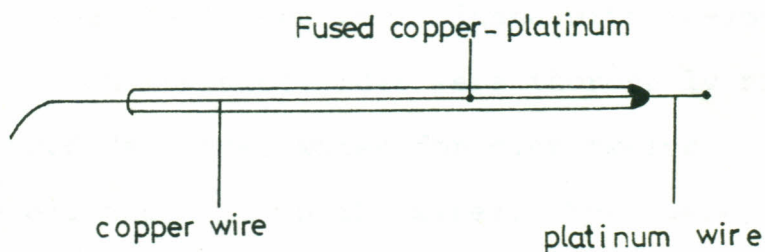


Fig. 3.3.1. The Electrode.

The surface area of the two pairs of electrodes usually prepared together was approximately 0.4cm^2 . The platinum wire was cleaned by a very fine polishing paper (grade 4/0), polishing in one direction only. This operation was not necessary for subsequent preparations.

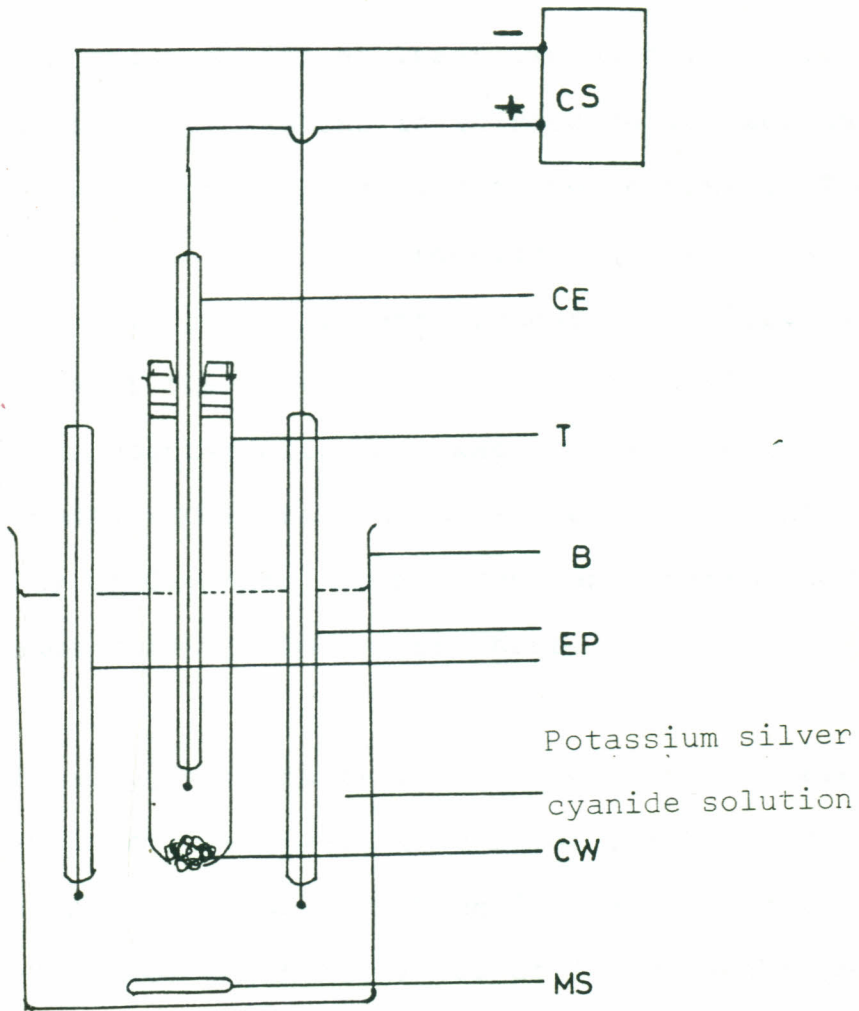
The general procedure followed for the preparation of electrodes was as that described by Ives and Janz (26), although with some modifications.

The electrodes were washed in boiling analytical grade concentrated nitric acid for a period of at least two hours. This was to remove any metallic impurity from the surface of the polished platinum wires. The electrodes were rinsed with de-ionized water. Then the electrodes were thoroughly rinsed in stirred deionized water for over twelve hours to remove all the acid on the wires. They were then ready for silver plating.

The potassium silver cyanide, $\text{KAg}(\text{CN})_2$, for making the silver-plating solution was made as recommended by Basett and Corbett (27). One per

cent (1%) solution of potassium silver cyanide in de-ionized water was used for electroplating. The arrangement for silver plating is as shown in Fig. 3.3.2. Initially dilute silver nitrate, AgNO_3 , was added dropwise to remove free cyanide by precipitation until a faint cloudiness was produced. Two pairs of electrodes were prepared at the same time. The electrodes under preparation were short-circuited and connected to the cathode while a simple platinum wire was used as the anode. The latter was encased in a test tube with a cotton plug to act as a scintered diaphragm. The cotton plug ensured that the products of the anode were not released into the bulk of the solution. This prevented poisoning of the electrodes as dark marks left on the electrode wires resisted chlorodisatation.

A current density of 1mAcm^{-2} from a constant current source (Philips Harris Limited, England) was used for silver-plating for a period of five hours. The solution was constantly stirred magnetically. The electrodes were rinsed with de-ionized water followed by washing in 25%



- CS - Current source.
- CW - Cotton Wool
- T - Test Tube with Cotton Wool.
- CE - Counter Electrode (Platinum).
- B - Beaker.
- MS - Magnetic stirrer.
- EP - Electrodes under preparation.

Fig. 3.3.2. - Arrangement for silver-plating of electrodes.

ammonia solution for at least two hours. This was followed by washing in stirred de-ionized water to remove ammonia for at least twelve hours. The chloridisation in 0.1M hydrochloric acid (HCl) was performed in a similar arrangement as in Fig. 3.3.2, but without the test-tube with a cotton plug. Platinum counter electrode was the cathode and the electrodes under preparation anode. A current density of 0.5mAcm^{-2} from a constant current source was used for a period of one hour.

Finally, the short-circuited electrodes were washed in stirred de-ionized water for at least three days. They were then equilibrated in the test-solution (0.1M NaCl) for at least twelve hours before testing. A bias potential of less than $\pm 0.01\text{mV}$ was obtained.

For electrodes which were to be reprepared the silver chloride layer was first removed by washing in 25% ammonia solution, followed by rinsing with distilled water and boiling in concentrated nitric acid for at least two hours. The other procedure followed is as already described.

3.4. Solutions:

The salt used for making solutions were of analytical grade (BDH chemicals; Poole England). A calibrated two litre volumetric flask was used to make six litres of IM stock solution of Lithium chloride (LiCl); Sodium Chloride (NaCl) and Potassium chloride (KCl). The other calibrated flasks were used in diluting the stock solution to the required concentrations. Distilled de-ionized water was used to make all the solutions.

3.5. Membranes:

The membranes used in the experimental work were: BDH cation exchange membrane (Na⁺ form) of thickness 0.12mm manufactured by BDH Chemicals Ltd., Poole England; Permaplex C-20 cation exchange membrane of thickness 0.8mm manufactured by the Permutit Company Ltd., London England; Nepton CR 61 AZL 065 of thickness 1.12mm and Nepton CR 61 AZL 183 of thickness 1.16mm. Both Nepton membranes are manufactured by Ionic Inc. Mass; U.S.A.

Large membrane pieces were first soaked in de-ionized water. From these small pieces of membranes of diameter 9mm were cut and equilibrated

in reference solutions of 0.1M sodium chloride, 0.1M Potassium chloride and 0.1M Lithium chloride. These solutions were changed several times for complete conversion of the membrane to the required form. The membranes were equilibrated for over one month before being put in the cell for experimental work.

3.6. Experimental Procedures:

3.6.1. Streaming Potential Measurement in Permaplex C-20:

The membrane pieces already equilibrated as described in section 3.5 were thoroughly washed in de-ionized water and equilibrated in experimental solution overnight (at least 12 hours).

At the beginning of the experiment, the membrane and the electrodes were put in place (fig. 3.2.1) The glass reservoirs were then filled with the same solution (as the cell) and adjusted to the required pressure level. The cell, the tubes and tube connections were checked for air bubbles before experiments were commenced. The pressure pulses of 4.5 seconds were applied immediately. The streaming potentials were recorded at pressure levels of 80, 100, 120, 140, and 160 cm heights of solutions. This was after square pulses could be obtained.

3.6.1.1. Repeat of streaming potential measurements
in Permaplex C-20:

One piece of equilibrated membrane was used for all the experiments in one particular system e.g. sodium chloride system. The membrane was thoroughly cleaned in de-ionized water and put in place in the cell. The cell was filled with experimental solution starting with 0.1M concentration and left for at least 12 hours to equilibrate. At the start of the experiment, the cell was filled with fresh solution and electrodes put in place. The glass reservoirs filled with the same solution and adjusted to the required pressure level. The whole system was left undisturbed for at least four hours. The pressure pulses lasting 4.5 seconds were then applied alternatively to the cell. Five to ten square pulses were recorded rapidly at pressure levels of 80, 100, 120, 140 and 160 cm heights of solutions. Without removing the membrane from the cell, the membrane was equilibrated for subsequent experiments and the above procedure repeated.

3.6.2. Streaming Potential Measurements in Nepton

CR 61 AZL 065 and Nepton CR 61 AZL 183:

Different equilibrated membrane pieces were used for each particular experiment. The membranes were equilibrated as described in section 3.5. The membranes were thoroughly washed in de-ionized water before being equilibrated in experimental solution overnight. At the beginning of the experiment, the membrane and the electrodes were put in place. The glass reservoirs (Fig. 3.2.2) were then filled with the same solution (as the cell) and adjusted to the required pressure level. The whole system was left undisturbed for at least four hours after which the streaming potentials were recorded rapidly at each pressure level. The streaming potentials were recorded at pressure levels of 80, 100, 120, 140 and 160 cm heights of solutions. Again pressure pulses lasted 4.5 seconds.

3.6.3. Streaming Potential Measurements in BDH Cation Exchange Membrane.

The membrane pieces were equilibrated as described in section 3.5. The membrane pieces were thoroughly cleaned in de-ionized water before being put in the cell. Two membrane pieces were mounted in the cell, the cell filled with 0.1M sodium chloride solution and electrodes put in place. The PVC tubings and glass reservoirs were also filled

with 0.1M sodium chloride and adjusted to the pressure level of 100cm of solution. The streaming potentials were recorded after the system had attained equilibration (approximately after three hours). The above process was repeated for three, four and six membrane pieces mounted in the cell with 0.1M sodium chloride solution and at the same pressure level of 100cm of solution and streaming potentials recorded.

The experiment was now continued with the six membranes mounted in the cell. The six membranes were not removed from the cell. They were used for all the experiments starting with the lowest concentration of 0.1M sodium chloride to the highest 1M sodium chloride solution.

The cell was filled with experimental solution starting with 0.1M concentration and left for at least 12 hours to equilibrate. At the start of the experiment, the cell was filled with fresh solution and electrode put in place. The glass reservoirs filled with the same solution and adjusted to the required pressure level. The whole system was left

undisturbed for at least four hours after which 5 - 10 pulses were recorded rapidly at each pressure level. For subsequent concentrations, the membranes were equilibrated inside the cell and the procedures repeated. The streaming potentials were recorded at pressure levels of 80, 100, 120, 140 and 160 cm heights of solutions. The pressure pulses lasted 4.5 seconds.

3.6.4. Addition of Silver Nitrate to Experimental Solutions:

It was noted that it was taking a longer period of time to reach equilibration at higher concentrations of the solutions. This was due to a drift in the potential of silver-silver chloride electrodes. The cause of this poor behavior at high chloride ion concentration was probably due to the appreciable solubility of silver chloride layer of the electrode at high halide ion concentrations (28) due to the formation of complexes of the type

$$\text{AgCl} + n\text{Cl}^- \rightleftharpoons \text{AgCl}^{n-}_{n+1}$$
 It was therefore found necessary to add a drop of silver nitrate to the experimental solution to shift the equilibrium
$$\text{AgCl} + n\text{Cl}^- \rightleftharpoons \text{AgCl}^{n-}_{n+1}$$
 to the left due to the common ion effect. Silver nitrate was added until a faint cloudiness appeared and this was for concentrations above 0.4M.

3.7. Measurements:

The streaming potential, $\Delta\phi$, as a function of time was measured by a D.C. differential voltmeter fitted with a potentiometric recorder. Typical streaming potential recorded are shown in Figs. 3.7.1, 3.7.2, 3.7.3, 3.7.4, 3.7.5, 3.7.6, 3.7.7, 3.7.8.

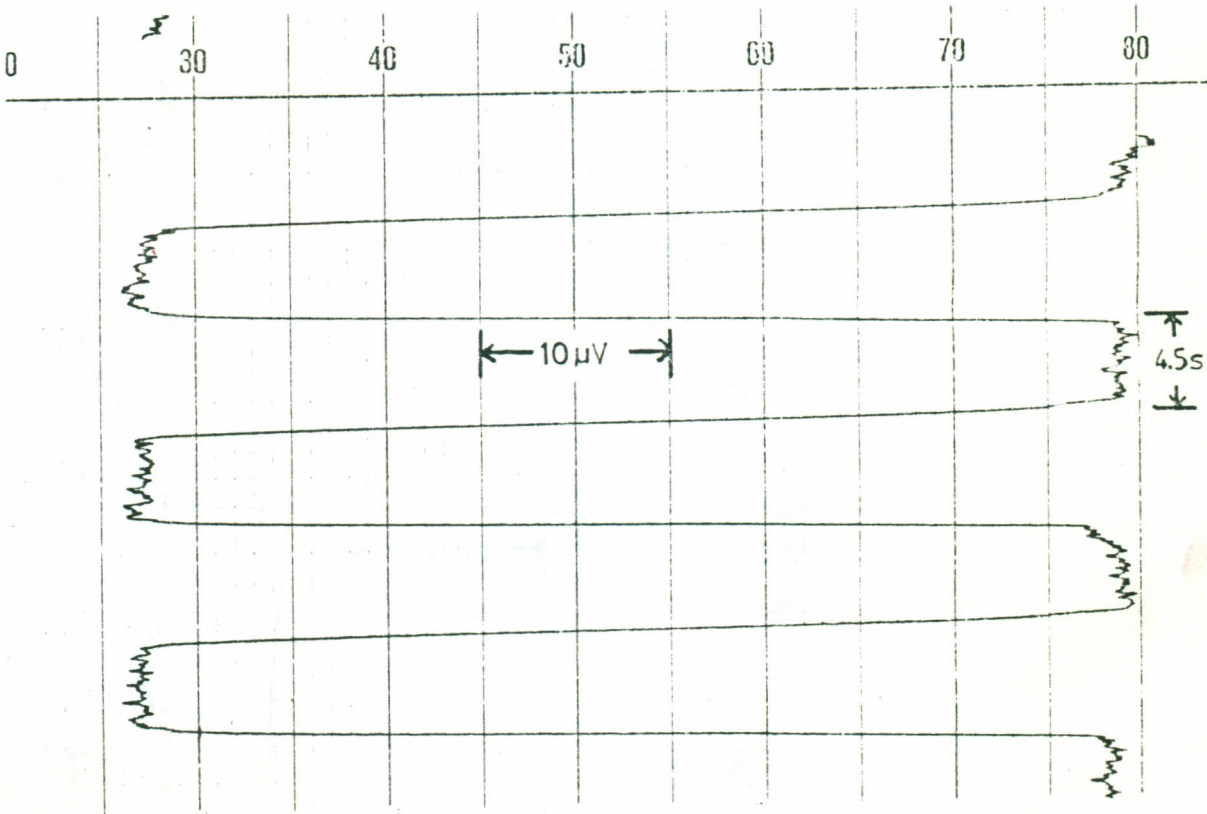
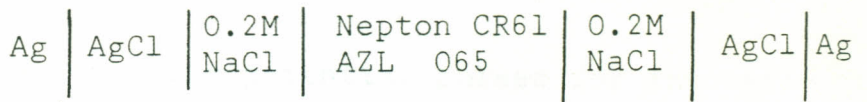


Fig. 3.7.1. - Streaming potential pulses for the cell



Pressure height 140 cm of solution.

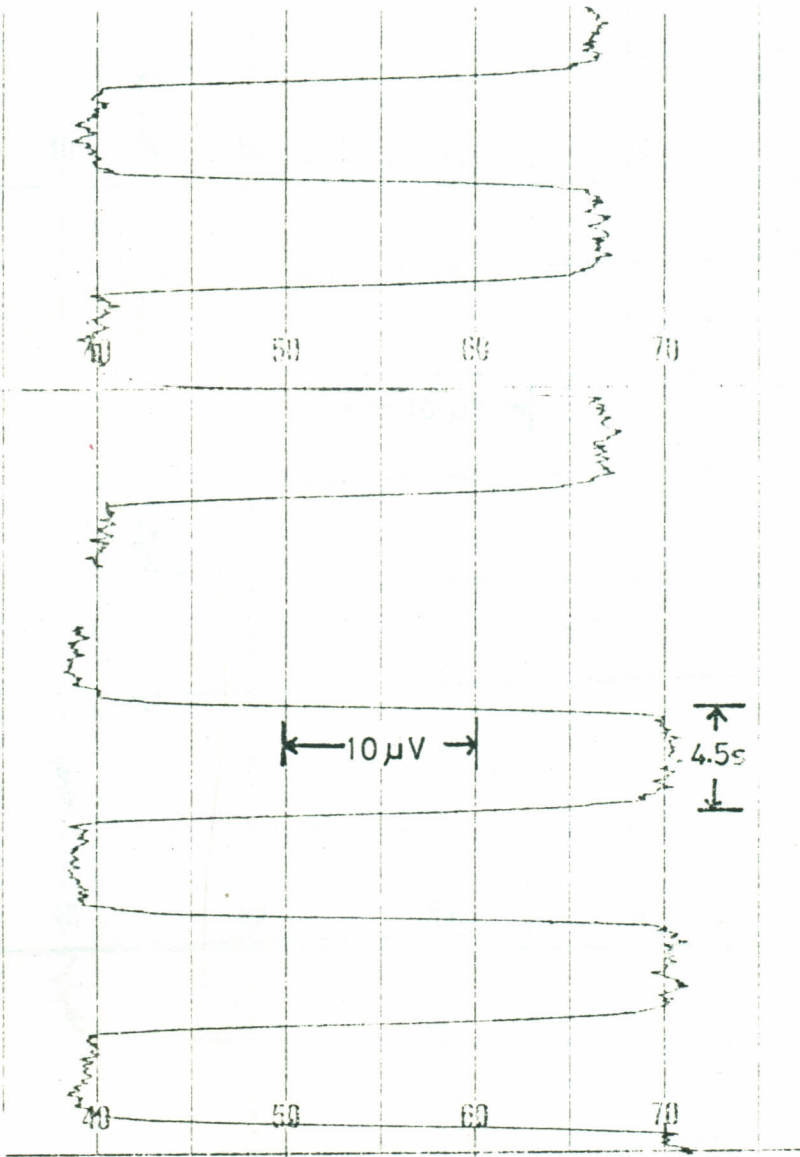
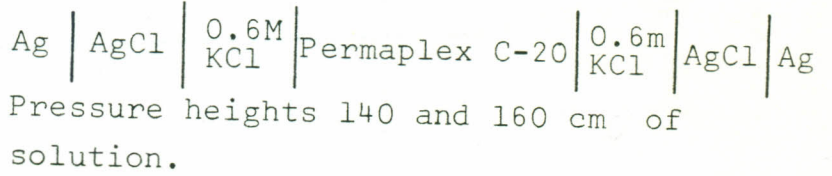


Fig. 3.7.2. - Streaming potential pulses for the cell



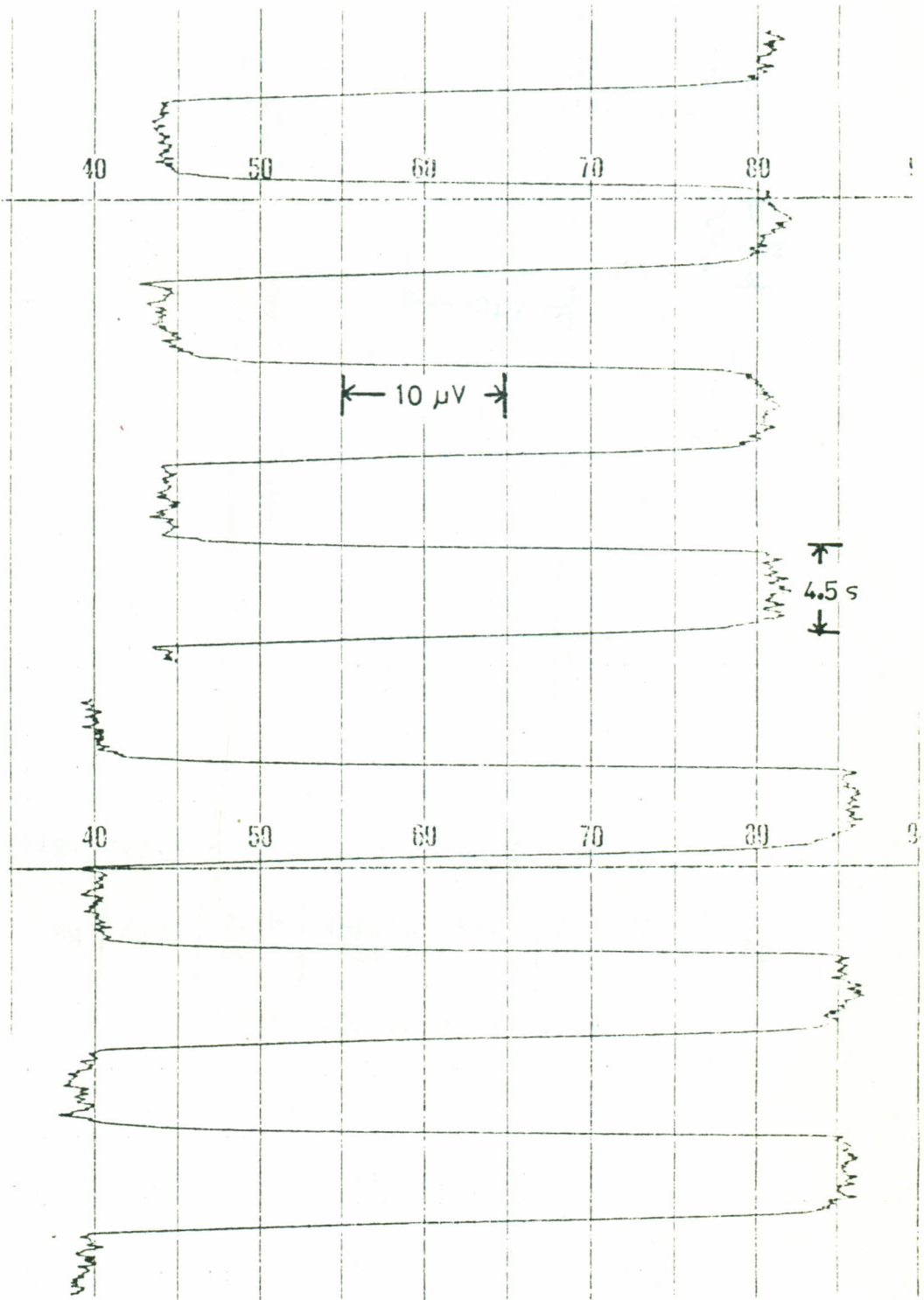


Fig. 3.7.3. - Streaming potential pulses for the cell



Pressure heights 80 and 100 cm. of solution.

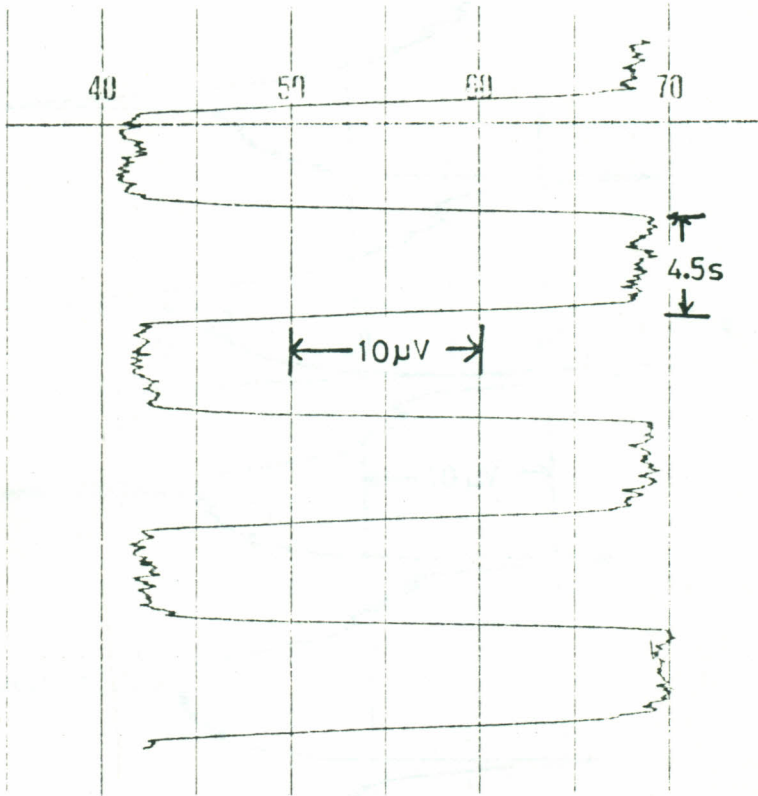


Fig. 3.7.4 - Streaming potential pulses for the cell



Pressure height 100 cm of solution.

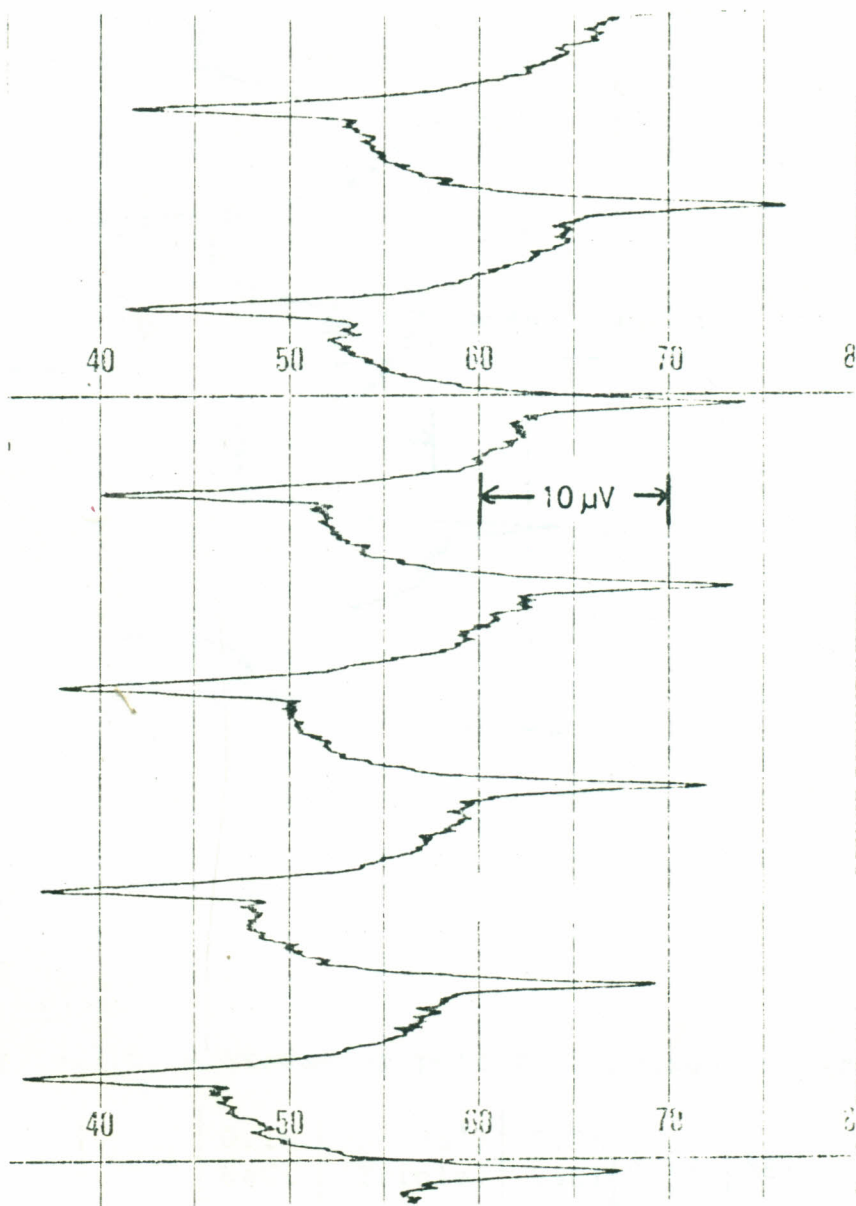
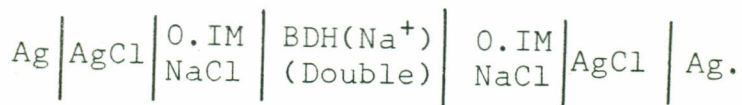


Fig. 3.7.5. - Streaming potential pulses for the cell



Pressure height 100 cm of solution.

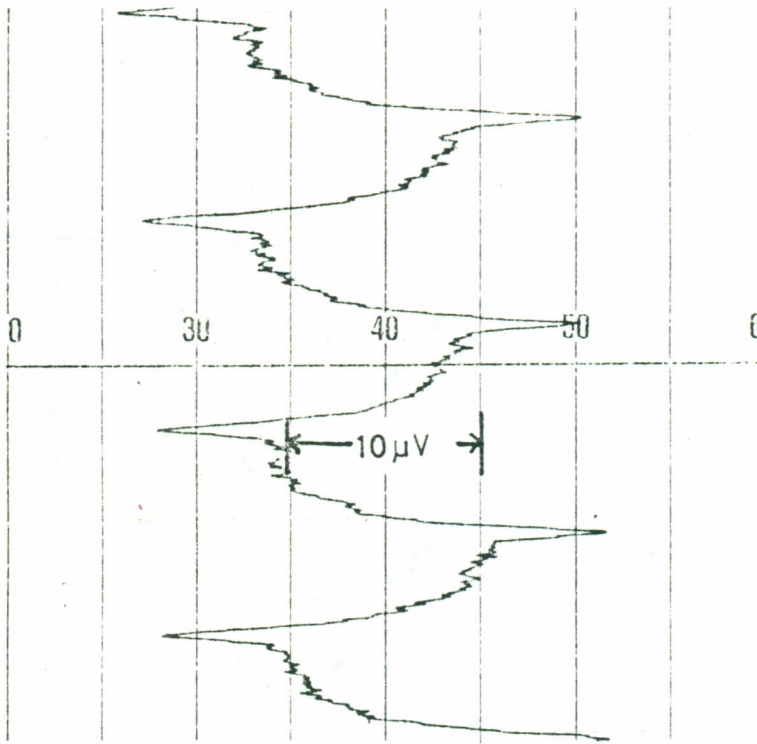
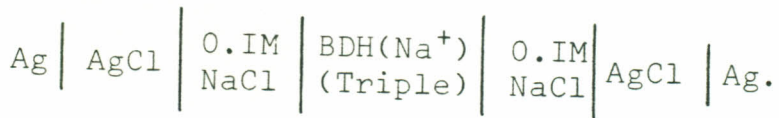


Fig. 3.7.6. - Streaming potential pulses for the cell



Pressure height 100cm of solution.

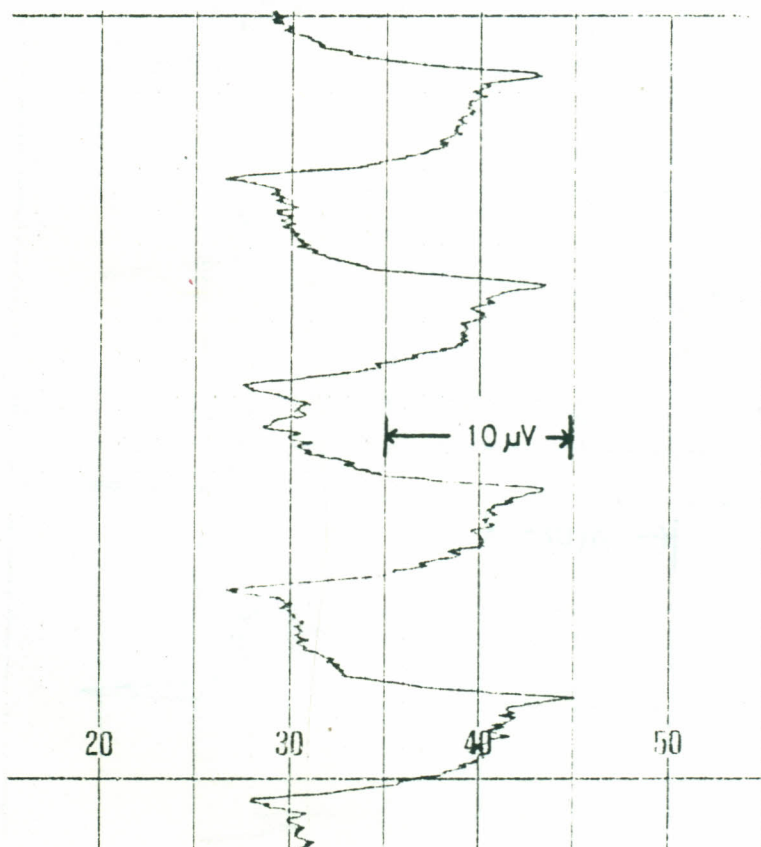
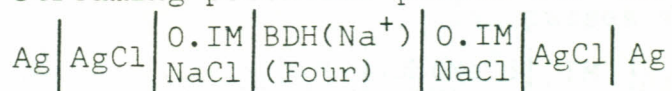


Fig. 3.7.7. Streaming potential pulses for the cell



Pressure height 100cm. of solution.

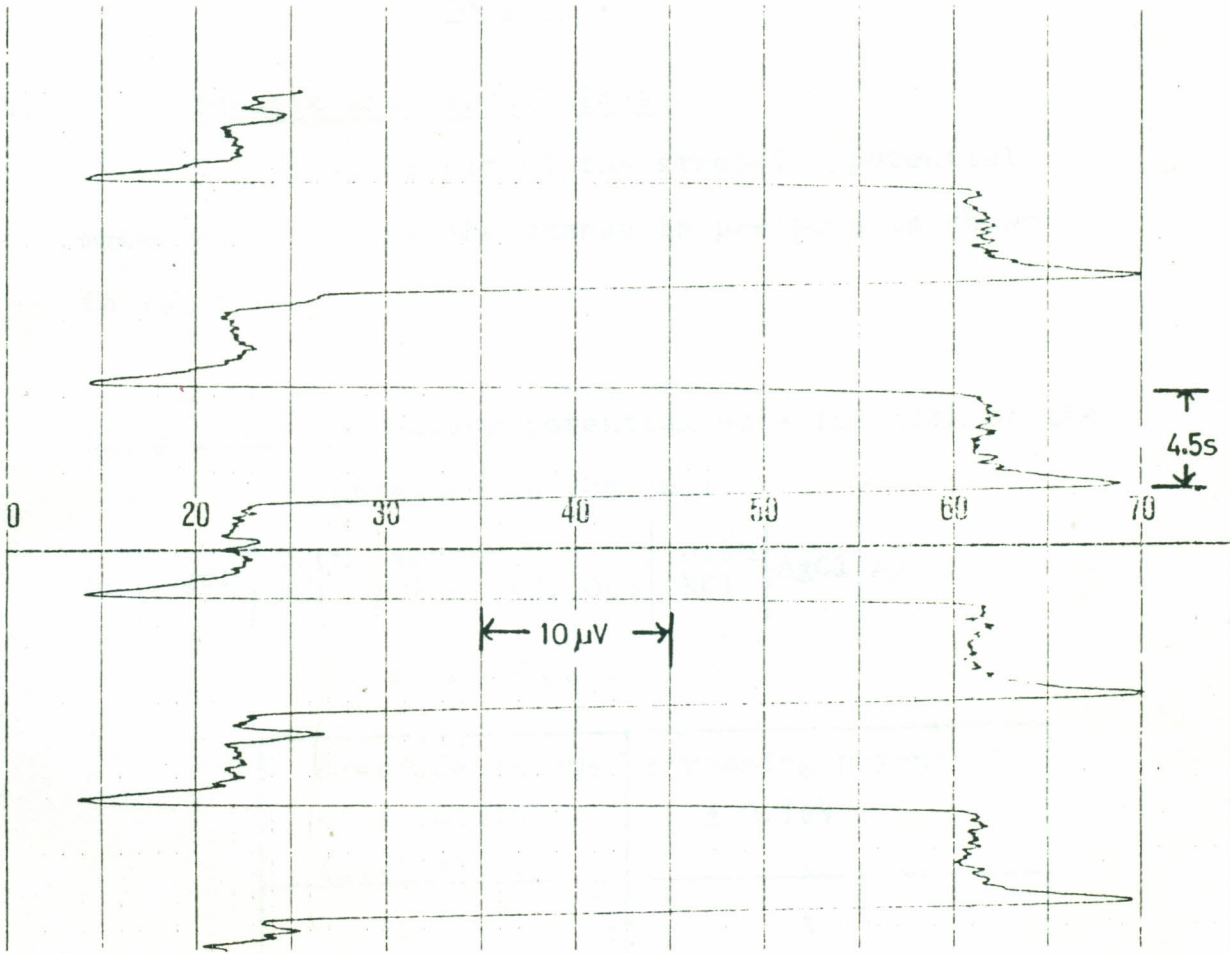
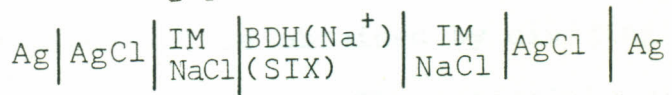


Fig. 3.7.8. Streaming potential pulses for the cell



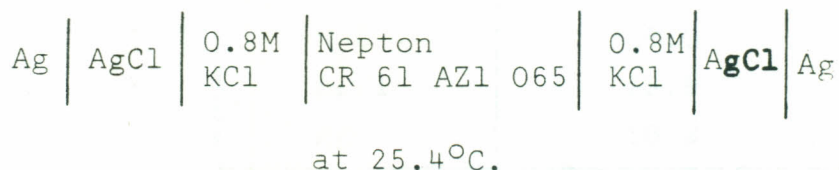
Pressure height 140cm of solution.

CHAPTER 4:

4. Results and Calculations:

A typical result of the streaming potential measurement versus the change in pressure is shown in Table 4.1.

Table 4.1: Streaming potential as a function of the pressure in the cell.



Pressure in cms of solution (±0.5cm)	streaming potential ± 0.1µV
80	9.5
100	12.0
120	14.7
140	17.1
160	19.7

The streaming potential is obtained by dividing the potential by a factor of two. The potentials are read from 5 - 10 square pulses recorded and an average value obtained. Figure 3.7.2 is a typical streaming potential pulse.

The transport numbers of water were calculated using Equation 2.3.13. Molar volumes of water V_{H_2O} , Silver V_{Ag} and Silver Chloride V_{AgCl} were obtained from the work of Andresen (29). The values are shown in Table 4.2.

Table 4.2: Molar volumes.

Substance	Molar volumes (cm^{-3})
H_2O	18.0
$AgCl$	25.8
Ag	10.3

Substituting for the Faraday, $F. = 96500 \text{ Cmol}^{-1}$, $V_{H_2O} = 18.0$, $V_{Ag} = 10.3$, $V_{AgCl} = 25.8$ and $\Delta\phi$ in volts equation (2.3.13) reduces to equation (4.1).

$$\frac{983.69 \times \text{gradient}(\mu V/cm)}{d(\text{gm cm}^{-3})} = - \left[\bar{V}_{MCl}^{-15.5} + \bar{t}_w \times 18.0 \right] \dots\dots\dots 4.1.$$

for all cation exchange membranes. The partial molar volumes \bar{V}_{MCl} , of different salts dissolved in water at a given concentration were calculated using the data reported by Harned and Owen (30). The calculated values of partial molar volumes, \bar{V}_2 at $25^\circ C$ are based on equation (4.2).

$$\bar{V}_2 = \bar{V}_2^0 + (3/2) S_v \sqrt{M} \dots\dots\dots 4.2.$$

where \bar{V}_2^0 is the apparent molar volume, M concentration

in moles per litre and S_v an experimentally determined constant specific for each electrolyte.

Table 4.3: Partial molar volumes of Lithium Chloride solutions at 25°C $\bar{V}_2^0 = 17.06$ and $S_v = 1.488$.

M	\bar{V}_2
0.1	17.7658
0.2	18.0582
0.4	18.4716
0.6	18.7889
0.8	19.0564
1	19.2920

Table 4.4: Partial molar volumes of sodium chloride solutions at 25°C $\bar{V}_2 = 16.61$ $S_v = 2.153$

M	\bar{V}_2
0.1	17.6312
0.2	18.0543
0.4	18.6525
0.6	19.1115
0.8	19.4985
1	19.8395

Table 4.5: Partial molar volumes of potassium Chloride solutions at 25°C $\bar{V}_2^0 = 26.81$
 $S_v = 2.327$.

M	\bar{V}_2
0.1	27.9138
0.2	28.3709
0.4	29.0176
0.6	29.5137
0.8	29.9319
0.1	30.3005

The value of the gradients ($\mu\text{V} / \text{cm}$) were obtained from the slope of a plot of streaming potential as a function of applied pressure. Figure 4.1 is a typical graphical presentation of the values in Table 4.1.

When pressure is applied in compartment one,

$\Delta P = P_2 - P_1 < 0$ and hence the value of the slope is negative.

The densities of the solutions were calculated from the data reported in International Critical Tables Vol. III (31). They are tabulated in Table 4.6.

Table 4.6: The densities of the solutions at 25°C.
in gm cm⁻³

M	Density of Lithium Chloride	Density of Sodium Chloride	Density of Potassium Chloride
0.1	0.9996	1.00116	1.00180
0.2	0.0020	1.00527	1.00653
0.4	1.0069	1.01351	1.01604
0.6	1.0118	1.02179	1.025560
0.8	1.0167	1.03013	1.03520
1	1.0215	1.03581	1.04491

Tables 4.7 and 4.16 show the gradients and calculated water transport numbers in different membranes and at different electrolyte concentrations. Figures 4.2 to 4.6 shows the graphical presentations of the dependence of water transport numbers on concentration for different membranes and different electrolytes.

Table 4.7: Gradients and calculated water transport numbers for Nepton CR 61 AZL 065 in Potassium Chloride solutions.

Concentration M	Gradients ($\mu\text{V}/\text{cm}$)	Standard error in gradient	Correlation Coefficient (r)	Water transport number (\bar{t}_w)
0.1	0.1985	0.0057	0.9974	10.1 \pm 0.3
0.2	0.1737	0.0036	0.9984	8.7 \pm 0.2
0.4	0.1478	0.0067	0.9938	7.2 \pm 0.3
0.6	0.1282	0.0128	0.9706	6.0 \pm 0.6
0.8	0.1276	0.0010	0.9998	5.9 \pm 0.1
1	0.1030	0.0120	0.9605	4.5 \pm 0.5

Table 4.8: Gradients and calculated water transport numbers for Nepton CR 61 AZL 065 in Sodium Chloride solutions

Concentration M	Gradients ($\mu\text{V}/\text{cm}$)	Standard error in gradient	Correlation Coefficient (r)	Water transport number(\bar{t}_w)
0.1	0.2220	0.0031	0.9994	12.0 \pm 0.2
0.2	0.1790	0.0069	0.9954	9.6 \pm 0.3
0.4	0.1680	0.0095	0.9905	8.9 \pm 0.5
0.6	0.1675	0.0044	0.9979	8.7 \pm 0.2
0.8	0.1589	0.0033	0.9987	8.2 \pm 0.2
1	0.1391	0.0016	0.9996	7.1 \pm 0.1

Table 4.9: Gradients and calculated water transport numbers for Nepton CR61 AZL 065 in Lithium Chloride solutions.

Concentration M	Gradients ($\mu\text{V}/\text{cm}$)	Standard error in gradients	Correlation Coefficient (r)	Water transport number(\bar{t}_w)
0.1	0.3616	0.0058	0.9992	19.6 \pm 0.3
0.2	0.3537	0.0133	0.9957	19.1 \pm 0.7
0.4	0.2975	0.0047	0.9992	16.0 \pm 0.2
0.6	0.2430	0.0068	0.9977	12.9 \pm 0.3
0.8	0.2233	0.0035	0.9993	11.8 \pm 0.2
1	0.2075	0.0024	0.9996	10.9 \pm 0.1

Table 4.10: Gradients and calculated water transport numbers for Nepton CR61 AZL 183 in Lithium Chloride solutions.

Concentration M	Gradients ($\mu\text{V}/\text{cm}$)	Standard error in gradients	Correlation Coefficient (r)	Water transport number(\bar{t}_w)
0.1	0.2140	0.0034	0.9992	11.6 \pm 0.2
0.2	0.2007	0.0165	0.9866	10.8 \pm 0.8
0.4	0.1594	0.0058	0.9959	8.5 \pm 0.3
0.6	0.1350	0.0020	0.9993	7.1 \pm 0.1
0.8	0.1046	0.0029	0.9977	5.4 \pm 0.1
1	0.0884	0.0018	0.9986	4.5 \pm 0.1

Table 4.11: Gradients and calculated water transport numbers for Nepton CR61 AZL 183 in Sodium Chloride solutions.

Concentration M	Gradients ($\mu\text{V}/\text{cm}$)	Standard error in gradient	Correlation Coefficient (r)	Water transport number (\bar{t}_w)
0.1	0.2220	0.0088	0.9952	11.9 \pm 0.5
0.2	0.1870	0.0088	0.9932	10.0 \pm 0.5
0.4	0.1618	0.0052	0.9969	8.5 \pm 0.3
0.6	0.1178	0.0032	0.9977	6.1 \pm 0.2
0.8	0.1061	0.0032	0.9972	5.4 \pm 0.2
1	0.0964	0.0045	0.9935	4.8 \pm 0.2

Table 4.12: Gradients and calculated water transport numbers for Nepton CR61 AZL 183 in Potassium Chloride solutions.

Concentration M	Gradients ($\mu\text{V}/\text{cm}$)	Standard error in gradients	Correlation Coefficient (r)	Water transport number(\bar{t}_w)
0.1	0.2309	0.0059	0.9980	11.9 \pm 0.3
0.2	0.1875	0.0127	0.9862	9.4 \pm 0.6
0.4	0.1645	0.0027	0.9992	8.1 \pm 0.1
0.6	0.1247	0.0071	0.9902	5.8 \pm 0.3
0.8	0.0909	0.0070	0.9825	4.0 \pm 0.3
1	0.0939	0.0020	0.9984	4.0 \pm 0.1

Table 4.13: Gradients and calculated water transport numbers for Permplex C-20 in Lithium Chloride solutions:

Concentration M	Gradients ($\mu\text{V}/\text{cm}$)	Standard error in gradient	Correlation Coefficient (r)	Water Transport number(\bar{t}_w)
0.1	0.1122	0.0071	0.9881	6.0 \pm 0.4
0.2	0.0829	0.0064	0.9825	4.4 \pm 0.3
0.4	0.0937	0.0062	0.9872	4.9 \pm 0.3
0.6	0.0925	0.0025	0.9978	4.8 \pm 0.1
0.8	0.0875	0.0025	0.9975	4.5 \pm 0.1
1	0.0750	0.0050	0.7141	3.8 \pm 0.2

Table 4.14: Gradients and calculated water transport numbers for Permplex C-20 in Sodium Chloride solutions.

Concentration M	Gradient ($\mu\text{V}/\text{cm}$)	Standard error in gradient	Correlation Coefficient	Water transport number(\bar{t}_w)
0.1	0.1250	0.0000	1.0000	6.7 \pm 0.0
0.2	0.1109	0.0044	0.9953	5.9 \pm 0.2
0.4	0.1190	0.0015	0.9995	6.2 \pm 0.1
0.6	0.1040	0.0035	0.9966	5.4 \pm 0.2
0.8	0.0983	0.0014	0.9997	5.0 \pm 0.1
1	0.1000	0.0000	1.0000	5.0 \pm 0.0

Table 4.15: Gradients and calculated water transport numbers for Permaplex C-20 in Potassium Chloride solutions

Concentration M	Gradient ($\mu\text{V}/\text{cm}$)	Standard error in gradient	Correlation Coefficient (r)	Water transport numbers(\bar{t}_w)
0.1	0.09399	0.0044	0.9934	4.4 \pm 0.2
0.2	0.1025	0.0047	0.9935	4.8 \pm 0.2
0.4	0.0950	0.0028	0.9972	4.4 \pm 0.2
0.6	0.0892	0.0020	0.9984	4.0 \pm 0.1
0.8	0.0890	0.0039	0.9953	3.9 \pm 0.2
1	0.0825	0.0119	0.9594	3.5 \pm 0.5

Table 4.16: Gradients and calculated water transport numbers for BDH(Na^+ form) - Six membrane in Sodium Chloride Solution.

Concentration M	Gradient ($\mu\text{V}/\text{cm}$)	Standard error in gradient	Correlation Coefficient (r)	Water Transport number (\bar{t}_w)
0.1	0.0845	0.0028	0.9966	4.5 \pm 0.1
0.2	0.0975	0.0062	0.9877	5.2 \pm 0.1
0.4	0.0898	0.0041	0.9938	4.7 \pm 0.2
0.6	0.1100	0.0028	0.9979	5.7 \pm 0.1
0.8	0.1338	0.0047	0.9963	6.9 \pm 0.2
1	0.1537	0.0097	0.9880	7.9 \pm 0.4

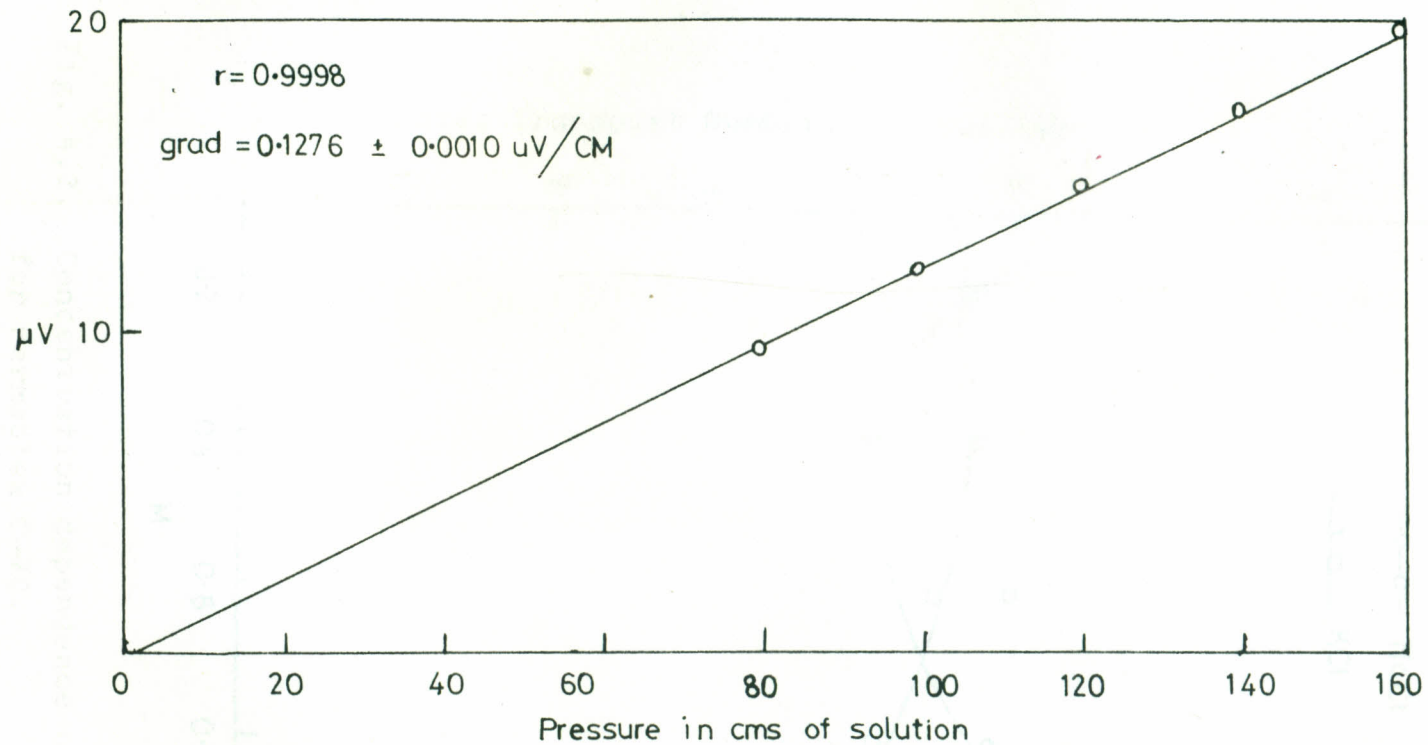


Fig. 4.1. streaming potential as a function of applied pressure in the cell



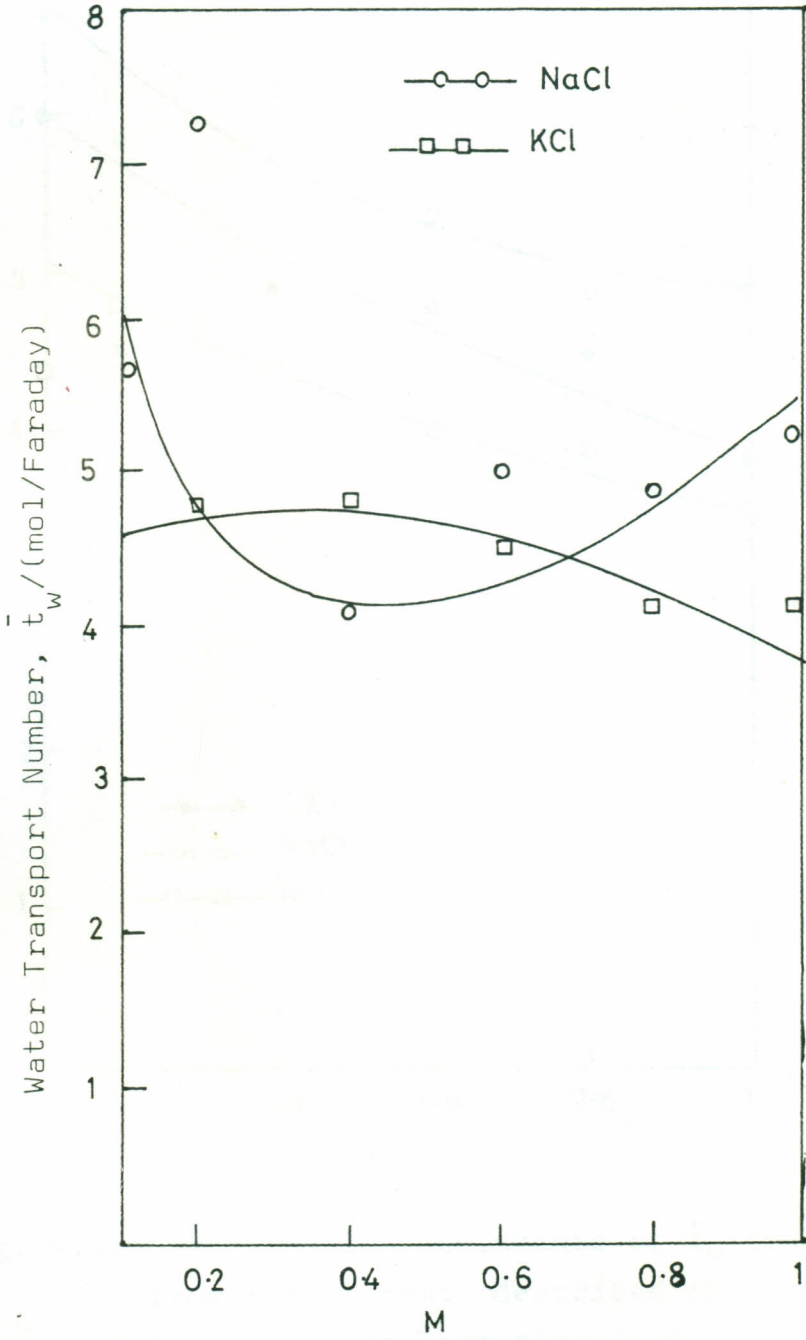


Fig. 4.2. Concentration dependence of \bar{t}_w (section 3.6.1) for Permaplex C-20.

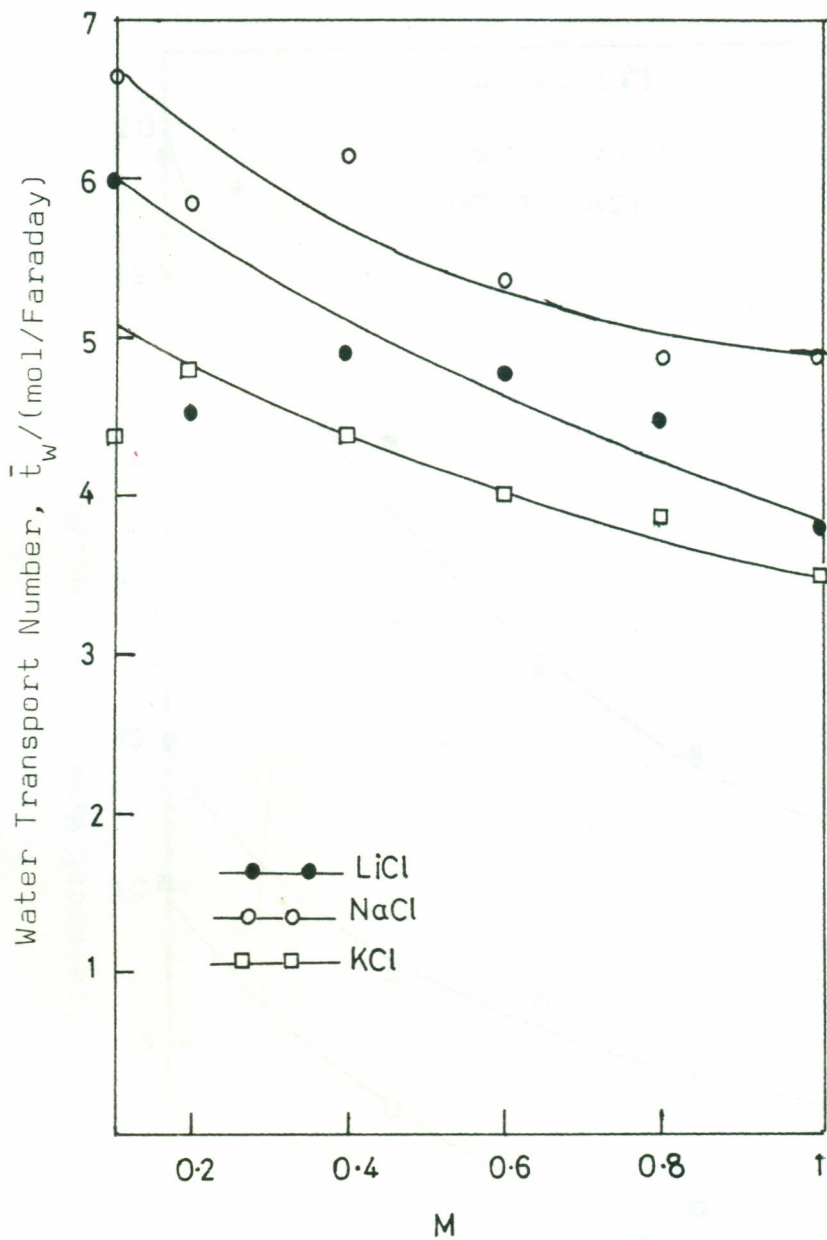


Fig. 4.3. Concentration dependence of \bar{t}_w (calculated from measurements described in section 3.6.1.1.) for Permaplex C 20.

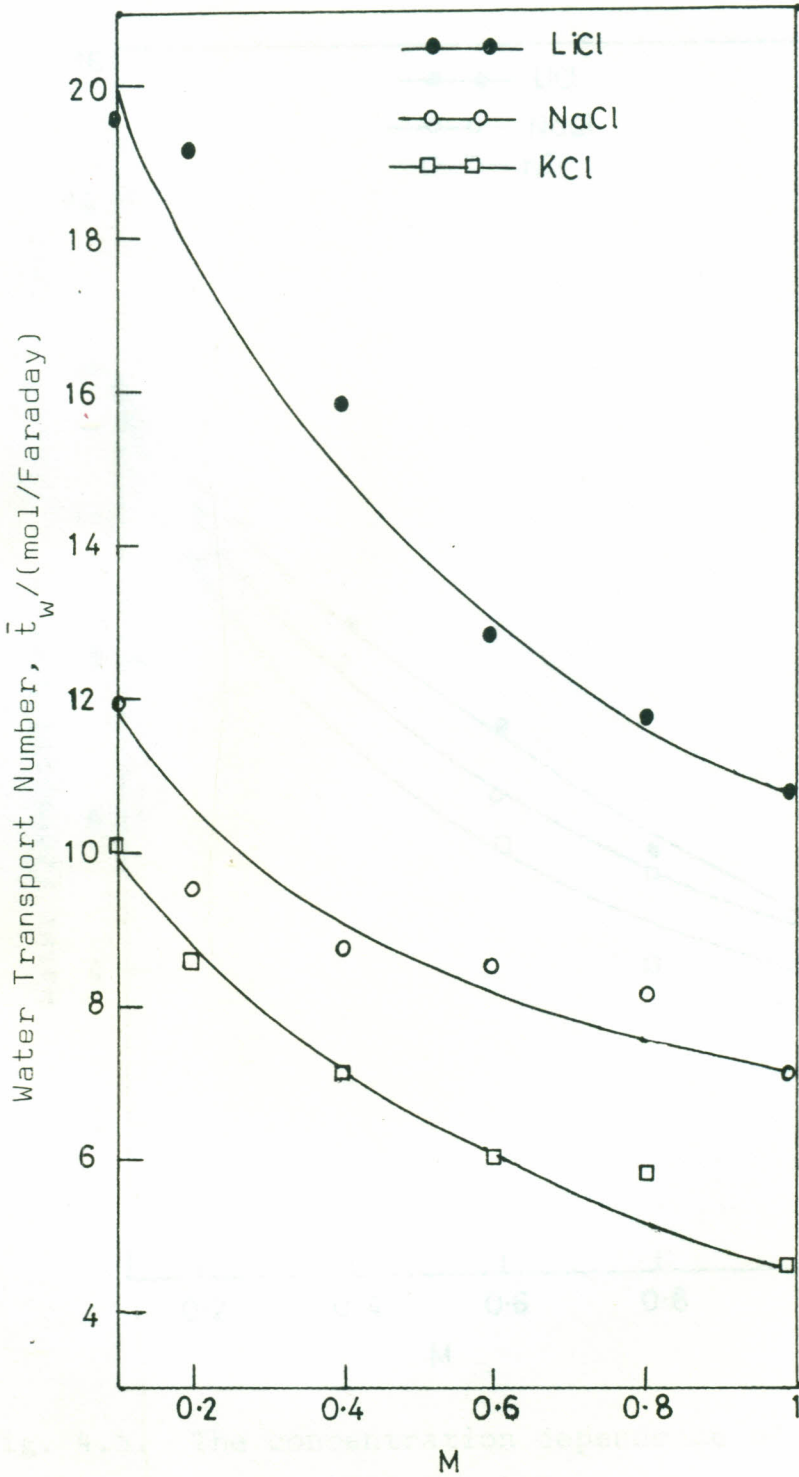


Fig. 4.4. The concentration dependence of water transport for Nepton CR61 AZL 065.

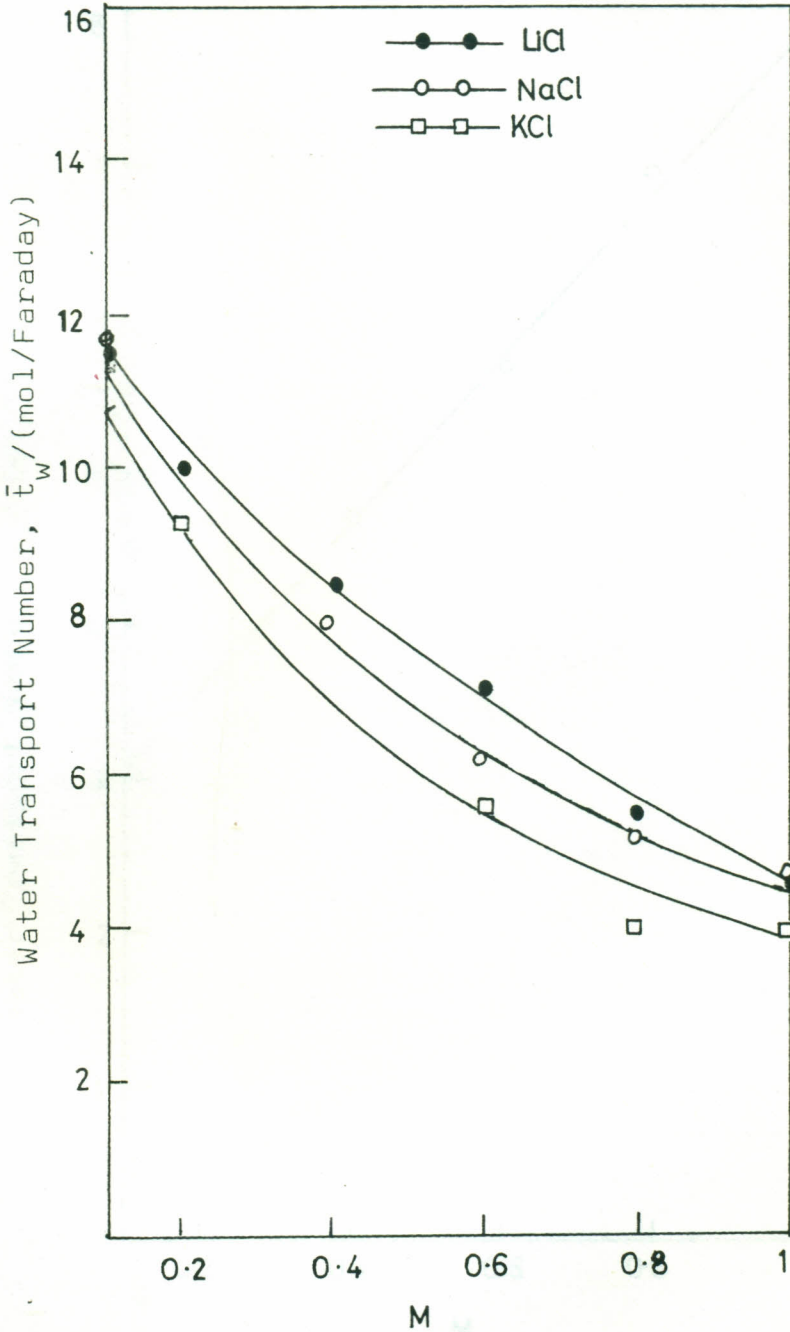


Fig. 4.5. The concentration dependence of \bar{t}_w for Nepton CR61 AZL 183.

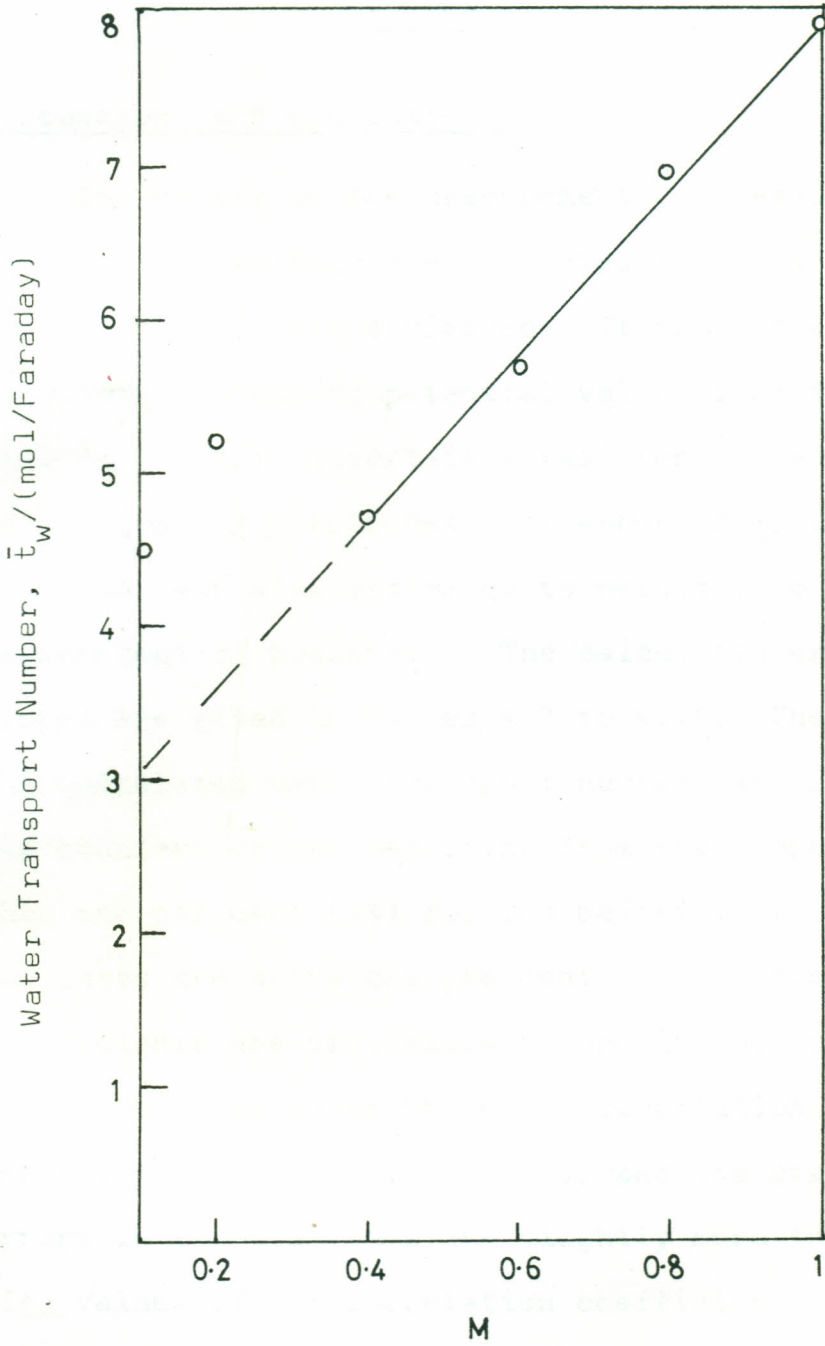


Fig. 4.6. The concentration dependence of \bar{t}_w in NaCl solutions for BDH(Na^+) (six membranes).

CHAPTER 5:

5. Discussion and Conclusion :

The errors in the measurement of pressure and streaming potentials are indicated in Table 4.1. The error of $\pm 0.1 \mu\text{V}$ was estimated. It shows the uncertainty of reading streaming potential values from the pulse records. This uncertainty was from the electrical noise from the electrodes. An error of $\pm 0.5 \text{ cm}$ of solution was also estimated to result from the measurement of pressures. The calculated errors of slopes are given in Tables 4.7 to 4.16. The errors in the calculated water transport numbers are also shown. The standard errors resulting from the slopes are less than one per cent (1%) for the majority of cases. A few cases are above one per cent. The correlation coefficients are very close to one in most cases. There are a few cases where the correlation coefficients are relatively low (i.e. 0.9605) and the standard errors in the gradients are slightly more than 1%. The high values of the correlation coefficients is an indication that the streaming potentials are linear functions of the applied hydrostatic pressures. It was also observed that streaming potential measurements require a sufficient equilibration time. This is illustrated in the plots of calculated water transport

numbers against concentration for Permaplex C-20 in Figures 4.2 and 4.3.

An important observation in the present work which agrees with observations by other investigators is that the water transport number (\bar{t}_w) decreases with increasing salt concentration (14). Figures 4.3 to 4.5 are the graphical representations of the concentration dependence of water transport numbers for different electrolytes. The cause of this effect is that the membrane cease to be selectively exchanging cations at high salt concentrations. When anions are present in the cation exchange membrane, water transport is reduced because anions and cations carry water in opposite directions.

In the present work, pressure pulses of upto 180cm of solution were applied during the streaming potential measurement. The pressure pulse lasted 4.5 seconds and it was applied alternatively on both sides of the cell. The streaming potential pulses were recorded rapidly. In this work, the applied pressures were approximately four times lower than those applied by Trivijitkasem, P. and Østvold, T. (4) in their work on determination of water

transport numbers across anionic and cationic exchange membranes. They applied square pulses of 200,400 and 600mm of mercury over a period of 60 seconds. This required a longer time for the cell to restore its equilibrium potential. It may be observed from Figure 5.1, where the emf is recorded versus time for the membrane AR 103 PZL 183 in 0.01N BaCl_2 that when a pressure pulse of 400mm of mercury is removed after one minute the cell slowly restores its original value.

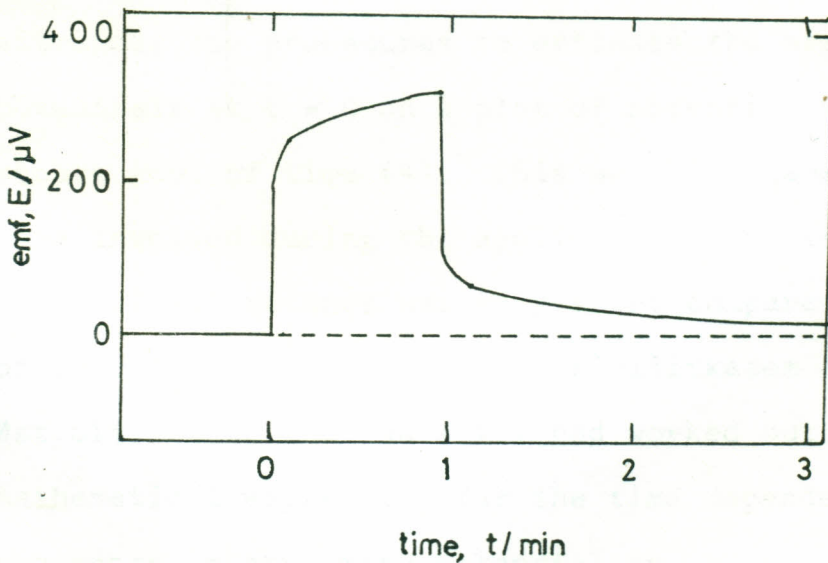


Fig. 5.1. The cell potential recorded as a function of time for the membrane AR 103 PZL 183 in 0.01N BaCl_2 with $\Delta P = 400\text{mmHg}$.

However, in this present work, lower hydrostatic pressures were applied over a short period of time. It is shown as in Fig. 3.7.3. that it was possible to get almost reproducible square pulses. There is a very small change in streaming potential within the short time of 4.5 seconds. The consequence of this is that the cell takes a much shorter time to restore its equilibrium position. It is therefore, expected that the measured streaming potentials are as close as possible to the true streaming potentials.

It was not found necessary to use graphical and extrapolation procedures to estimate the streaming potentials at $t = 0$ on a plot of potential versus square root of time (4). This was so because the time involved during the application of pressure pulse of 4.5 seconds was very short compared to that of 60 seconds in the work of Trivijitkasem and Østvold. Brun and Vaala (3) had worked out a mathematical expression for the time dependence of the apparent streaming potential as

$$-\left(\frac{\Delta\phi'}{\Delta P}\right) = \Delta\phi + A\sqrt{\frac{Dt}{\pi}} \dots\dots\dots 5.1$$

Here A is a constant, $\Delta\phi$ is the true streaming potential, t the time, π the number π and D is the

salt diffusion coefficient. Equation 5.1 shows that the measured (apparent) streaming potential, $\Delta\phi'$, approaches the true streaming potential, $\Delta\phi$, as the value of time, t , approaches zero. In this present work, the value of time, t , as estimated from the graphical pressure pulses recorded was made as small as possible and so it is expected that the measured streaming potentials were as close to the true streaming potential as possible. Hence the calculated water transport numbers are expected to be more reliable.

A major source of error in streaming potential measurement can be the membrane concentration contribution

$$E_c = RT \ln \left(\frac{C_2(t)}{C_1(t)} \right) \quad \dots \quad 5.2$$

where E_c is the membrane concentration potential, $C_2(t)$ and $C_1(t)$ are the concentration at the membrane surface at time, t . From equation 5.2 if $C_2(t) = C_1(t)$ then the membrane concentration potential contribution is zero. From the work of Brun, the concentrations at the membrane surfaces are functions of time given by

$$C(o, t) = C_o \left[I - \frac{1}{\sqrt{\pi}} \left(v \sqrt{\frac{t}{D}} \right) + \frac{1}{8} \left(v \sqrt{\frac{t}{D}} \right)^2 \dots \dots \dots 5.3 \right]$$

Equation 5.3 is a solution for the high pressure side of the membrane and v , the streaming velocity, is negative. If t is zero, then $C(0,0) = C_0$, the concentration of the bulk of solution. By applying the short hydrostatic pressures alternatively on both sides of the cell, it is expected that electrolyte accumulation on the high pressure side and depletion on the low pressure side that would lead to different concentrations at the membrane surface at time t is avoided. It is, therefore, reasonable to assume that the membrane concentration potential difference contribution to the measured streaming potential is negligible.

In agreement with other workers it is observed that the calculated water transport numbers at a given salt concentration decreased in the order $K < Na < Li$ as shown in Figures 4.4 and 4.5. This is partly as a result of the degree of hydration of the given ions with Lithium ion being the highly hydrated while potassium ion the least. Thus Lithium ion carry along with it more water molecules. However, the calculated water transport numbers in Permaplex C-20 at a given concentration of the electrolytes decreased in the order $K < Li < Na$, Wallevik (32) had

observed that sometimes the streaming potential measured varied with different membrane clamping pressure for Potassium Chloride and Lithium Chloride electrolytes with Permaplex C-20 membranes. Thairu (22) on the other hand did not observe the effect of varying clamping pressure. It is anticipated that further work with Permaplex C-20 and with Potassium Chloride and Lithium Chloride electrolytes would be carried out.

Attempt was made to determine the water transport numbers across the thin BDH(Na^+) cation exchange membrane. This was done by increasing the thickness of the membranes by mounting several pieces in the cell. The streaming potential pulses are shown in Figures 3.7.5, 3.7.6., 3.7.7 and 3.7.8 for double, triple, quadruple and six membrane pieces mounted in the cell respectively. Kamiti, F.M. (33) working with the same membrane, BDH(Na^+), and using the emf method had shown that the water transport numbers across the membrane do not vary with increasing concentration of the electrolyte used. Figures 3.7.5, 3.7.6, 3.7.7 and 3.7.8 also shows the effect of increasing the number of membrane pieces mounted in

the cell on the measured streaming potentials. It is noted that the heights of the sharp peaks decreases with increasing number of membrane pieces mounted together. It is observed that the calculated water transport numbers increases linearly with increasing concentration of sodium chloride (Fig. 4.6). As seen in Figures 3.7.5 to 3.7.8, streaming potentials were actually recorded but it is not clear from the literature how the existence of the thin liquid films between the membranes could affect the streaming potentials and hence the water transport numbers. The result is not consistent with what has been reported in the literature. It is expected that more work with thin membranes will be carried out. The streaming potential method is yet not a good method for the determination of water transport numbers in thin membranes. One limitation of the streaming potential method as discussed by Trivijitkasem and Østvold is that very thin membranes give poor reproducibility due to stretching and deformation of the membrane when pressure is applied. This they observed for NA 20 and NC 20 membranes which are both very thin.

A P P E N D I C E S:

A.1. Calculation of densities of electrolyte solutions at 25°C.

Densities of different concentration of electrolytes was calculated from the data reported in "International Critical Tables Vol. III" (31). The quantities reported in the tables are temperature in °C, Weight (wt)% of the solute, and the density of the solution in g/ml.

The concentration in wt % of the solute was converted to concentration in moles per litre (M). For example the concentration in moles per litre of 1% sodium chloride solution (Molecular Weight of NaCl = 58.44g) was calculated as follows.

100g of solvent contains 1g of NaCl(solute)
Then 1000g (≡ 1000ml) of solvent contains 10g of NaCl.

Hence 1% sodium chloride $\equiv \frac{10}{58.44} \approx 0.1711M$
sodium chloride.

Table A.1.1 - Densities of LiCl solutions
at 25°C.

Molecular weight 42.4g

LiCl

%	M(calculated)	D_4^{25}
1	0.2358	1.00292
2	0.4717	1.00870
4	0.9434	1.02019
6	1.4151	1.03161

Table A.1.2 - Densities of NaCl solutions
at 25°C.

Molecular weight 58.44g

NaCl

%	M(calculated)	D_4^{25}
1	0.1711	1.00409
2	0.3422	1.01112
4	0.6845	1.02530
6	1.0262	1.03963

Table A.1.3 - Densities of KCl solutions
at 25°C.

Molecular weight 74.55g

KCl

%	M(calculated)	D_4^{25}
1	0.1341	1.00342
2	0.2683	1.00977
4	0.5365	1.02255
6	0.8048	1.03544
8	1.0731	1.04837

Linear interpolation technique was employed
to calculate the densities at other
concentrations.

REFERENCES:

1. Saxen, U. Ann. Physik 47 46 (1892).
2. Mazur, P. and Overbeek, J.T.G. Rec.Trav.Chim 70 83 (1951).
3. Brun, T.S. and Vaala, D. Ber Bunsenges Physik Chem. 71 824 (1967).
4. Trivijitkasem, P. and Østvold, T., Electrochimica Acta 25 172 (1980).
5. Førland, T. and Thulin, L.V. "The potential across a membrane" Acta. Chem. Scand 22 3023 (1968).
6. Førland, T. Thulin, L.V. and Østvold, T. "Concentration cell with liquid junction." J. Chem. Ed. 48 741 (1971).
7. Lakshminarayanaiah, N., Transport Phenomena in artificial membranes Chem.Rev. 65 491 (1965).
8. Rosenberg, N.W., George, J.H.B., and Potter, W.D., J. Electrochem. Soc. 104 111 (1957).
9. Schulz, G., Z. anorg allgem. Chem. 301 97 (1959).
10. Oda, Y. and Yawataya, T., Bull. Chem. Soc. Japan 28 263 (1955)
11. Winger, A.G., Ferguson, R., and Kunin, R., J. Phys. Chem. 60 556 (1956).
12. Kressman, T.R.E., Stanbridge, P.A., Tye, F.L., and Wilson, A.G., Trans. Faraday Soc., 59 2133 (1963).
13. Tombalkian, A.S., Barton, H.T., and Graydon, W.F., Can. J. Chem. Eng., 42 61 (1964).
14. Lakshminarayanaiah, N., and Subrahmanyam, V. J. Phys. Chem. 72 1253 (1968)
15. Mussini, Torquato; Longhi, Paulo Chim. Ind. 57(2) 97-8 (1975).

16. Helfferich, F. "Ion Exchange." P. 392
McGraw Hill, New York (1962)
17. Schmid, G. and Schwarz, H. Z. Electrochem. 56
35 (1952).
18. Schmid, G. and Schwarz, H. Z. Electrochem 56
181 (1952).
19. Stewart, R.J. and Graydon, W.F. J. Phys. Chem. 61
164 (1957).
20. Henderson, R.M; J. Phys. Chem. 70 2694 (1966).
21. Brun, T.S. "Streaming Potential" Arbok Univ. i
Bergen Natur. V.r Nr.8, (1957).
22. Thairu, H.M., "PHD Thesis" University of
Trondheim, Norway, (1975).
23. Onsager, L. "Reciprocal relation in irreversible
processes I" Phy. Rev. 37-405 (1931).
24. Wilson, C.L. and Wilson, D.W. (Ed) Comprehensive
Analytical Chemistry Elsevier (1959) pp. 135.
25. Stewart, R.J. and Graydon, W.F., J. Physic Chem.61
164 (1957).
26. Ives, D.J.G. and Janz, G.J., "Reference electrodes,
theory and practice" Academic Press, London (1961).
27. Basett, H. and Corbett, A.S. "A phase rule study
of the cypro⁻, Argento, Auro⁻ and Thallo -
cyanides of potassium" J. Chem. Soc., 1672 (1924).
28. Luehrs, D.C; Iwamoto, R; and Kleinberg, J.
Inorg. Chem. 5 201 (1966).
29. Andresen, I.L., "Thesis" Division of Physical
Chemistry. The University of Trondheim, Norway
(1973).

30. Harned, H.S. and Owen, B.B. The Physical Chemistry of Electrolyte solutions 2nd edn. pp. 376 Reinhold, New York (1950).
31. International Critical Tables Volume III McGraw Hill Book Company.
32. Wallevik, O. "Transport number of Water in a Permaplex C 20 cation Exchange Membrane with alkali halides." Diploma Project. Division of Physical Chemistry, University of Trondheim Norway - 1973.
33. Kamiti, F.M. Personal Communication. (1987).